BC hydro

Peace River Project Water Use Plan

Title: A Feasibility Study for the Development of a RADARSAT-2 Dust Prediction System

Reference GMSWORKS-20

Implementation Year 4

A Feasibility Study for the Development of a

RADARSAT-2 Dust Prediction System: 2012 Annual Report

Study Period: January 1, 2012 – February 17, 2013

Dr. W.G. Nickling
Dr. J.A. Gillies
Ms. J. Guerra

Nickling Environmental Ltd.
Cambridge, Ontario

August 22, 2013

TABLE OF CONTENTS

EXECUTIVE SUMMARY

In the spring of 2009 a project was initiated to assess the feasibility of developing a model to identify the dust emission potential of beaches around the Williston Reservoir in relation to textural, surficial and meteorological conditions. This objective was fulfilled with the development of the WE_DUST_EM model. WE_DUST_EM uses relatively few input parameters and the methodology developed to obtain these input parameters using *in situ* measurements of emission potential (from PI-SWERL), GIS, and remote sensing techniques along with a stochastic approach for assessing threshold shear velocity. This model can aid in the development of an operational plan on when and where to apply dust control measures to maximize the investment on reducing the PM_{10} concentrations that impact the local and regional environment, while saving costs related to mitigation efforts.

In 2012-2013 a second type of model, the Lagrangian Particle Dispersion Model (LPDM) was also evaluated for its potential to inform management decisions through its capability to identify the frequency and magnitude of PM_{10} contributions to an identified receptor site (e.g., Tsay Keh village). This information can also be used to guide management decisions as it can identify which beaches contribute significantly or minimally to a defined receptor site. This can be defined on an event basis or at a broader temporal scale, for example, based on a characterization of dust event climatology for the Williston Reservoir. A dust event climatology defines the range of meteorological conditions that give rise to dust events and their frequency of occurrence. Combining a dust event climatology with the LPDM could provide a means to identify which beaches most impact a receptor in terms of the magnitude of the impact and the probability or frequency of occurrence of that impact. A receptor site can be defined based on a number of criteria including, for example, population density (Tsay Key village) or areas of special interest or concern (near reservoir camping areas).

For both models there are limits to the accuracy of their predictions that are a function of their inherent assumptions on characterizing the threshold of entrainment of dust and sand and the dust emission relationships in the case of the input for WE_DUST_EM, and the dispersion and deposition processes in the LPDM. A greater impact on model performance in either model is the very limited availability of meteorological data that characterize the wind fields within the Williston Reservoir and the patterns of PM_{10} concentration. New near-surface meteorological and PM_{10} data obtained via the established air quality monitoring network will improve the predictive capacity of the models, but critically important measurements of the conditions of the upper air environment are lacking. Upper air measurements of atmospheric stability and turbulent kinetic energy are critical for accurate estimates of particle dispersion and deposition within the LPDM. The prediction of shear velocity to drive the dust emission model is limited by

the very small data set from the tillage trials that measured aerodynamic roughness length for only Davis beach. Aerodynamic roughness is a characteristic of the surface that is required for estimating wind shear velocity. Based on the range of physical roughness observed on the beaches, which was quite limited (except where stumps are present), aerodynamic roughness likely changes within one order of magnitude across the beaches, so this is less a cause of uncertainty than other sources (e.g., wind speed, wind direction, stability, etc.). If modelling is to be advanced as a means to aid in dust mitigation planning it will be critical to improve the quality of the meteorological data for model inputs. Several options can be pursued: 1) use available modeled meteorological data available from Environment Canada, 2) develop a prognostic wind field model for the Williston Reservoir using available models (e.g., MM5/WRF), and 3) install additional instrumentation for corroborating model-predicted meteorological quantities.

In order to develop strategies and inform management decisions to reduce PM_{10} dust emissions from Williston Reservoir beaches it was necessary to develop an understanding of the dust emission potential for the beaches including the strength of the emissions and how they vary as a function of location and through time. This information also represents critical data inputs for the models WE_DUST_EM and the LPDM. This study used the Portable In-Situ Wind Erosion Laboratory (PI-SWERL) to estimate the critical wind shear velocity that initiates the movement of sand and the emission of dust (u_{*t}, m s^{-1}). Wind shear velocity (u_*, m s^{-1}) is the critical atmospheric parameter that drives wind erosion and dust emission. PI-SWERL was also used to directly measure the relationship between dust flux (F, µg m^{-2} s^{-1}) and u_*, m s^{-1}. PI-SWERL applies a known shear velocity to the beach surface and based on measurements of PM_{10} concentration and volumetric flow through the instrument estimates F. Application of multiple shear velocities allowed for the development of beach-specific emission potential relationships. Along with PI-SWERL measurements, samples of the beach sediments were collected for soil texture (i.e., quantification of % sand, % silt, and % clay composition) and moisture content (ratio of H_2O mass : sediment mass) measurements as both are known to affect emission strength. The emission potential relationships were extrapolated to beaches where PI-SWERL measurements were not made based on their mapped textural qualities determined by application of a simple algorithm relating reflectance to particle size applied to LandSAT data.

Over the course of the four years of this project sediment texture, PI-SWERL and moisture content measurements were collected for 20 different beaches at the Williston Reservoir. The measurements of soil texture show that there is year-to-year variation in the relative proportions of sand, silt, and clay in the top few centimetres of beach sediments. It is likely that these changes, in part, explain the observed variability in the dust emission potential as revealed by the PI-SWERL measurements. PM_{10} emissions changed between 2009 and 2012, for beaches measured in all four years (i.e., Davis and Collins), between a factor of three to nine

for the highest applied shear velocity (i.e., u_*=0.46 m s^{-1}). Other beaches showed very consistent emission potential relationships (e.g., Pete Toy, Shovel). Several reasons can be advanced as to what causes this year-to-year variability in emission potential. Cooler and moister conditions (i.e., higher RH) such as those that prevailed in 2011 likely caused reduced emissions. Another cause is likely related to the observed changes in soil texture. The clay component of the sediment is the critical reservoir of the PM_{10}. At this time however, the cause of the variability in soil texture that controls, in part, dust emission variability remains unknown. It is hypothesized that this variability is controlled by the phase of deposition of fine sediments through the water column following high pool and thereafter during the draw down phase. The control on the depositional process is likely a complex interaction between the amount of fine particles delivered to the reservoir by the rivers and streams, as well as bank erosion inputs, and the subsequent transport of these suspended particles to the different beaches by wind driven currents in the reservoir and their interaction with the bathymetry of the reservoir and the near shore environment. To gain an understanding of the spatial distribution patterns of the depositional flux of suspended sediments in the water column to the beaches a measurement program is recommended. This information would be useful in developing and understanding of which beaches have an increased probability of receiving silt and clay from the reservoir waters and aid in the decision making process to prioritize where mitigation should be focused to maximize the potential for reducing dust emissions.

The four years of emission potential measurements obtained with the PI-SWERL indicate that, even taking the observed variability into account, there are beaches that have a consistently higher emission potential than others. Consistently high emission beaches are: Shovel, Tsay Key, Davis N, Middle Creek N, Middle Creek S, and Collins. Other high emitting beaches based on one year of measurement were: Ruby Red, Lafferty, Bevel, Davis S, and Chowika. These data suggest that due consideration be given to prioritizing mitigation treatments to those beaches listed in the first grouping. In addition, due to the proximity of Tsay Keh village to the potentially high emitting Tsay Keh beach it is suggested that this beach always be afforded a high priority for application of dust mitigation methods. This is supported further by the LPDM results that consistently identify the Tsay Keh beach as the significant contributor to PM_{10} in the defined receptor-zone, i.e., a 2 km^2 area with the village in its centre.

The results of this study further confirms the efficacy of the PI-SWERL as a cost effective instrument for the measurement of both threshold shear velocity that defines the initiation of wind erosion and dust emission and develop the relationship between shear velocity and dust flux for sites with great economy of labour and logistics, as compared with more traditional methods such as tower-based or large portable wind tunnel measurements. PI-SWERL testing provided a means to constrain the temporal and spatial range of variability of dust emission potential, which was previously unknown for this area. Although it must be noted that a four

year record is still quite limited in terms of the uncertainty that the measurements have captured the full variability of the dust emission system. Coupling the measured dust emission data with the WE_DUST_EM and LPDM models provides a feasible PM_{10} emission prediction system, which can be used as a management tool to guide the dust control measures that will reduce the impacts of these emissions on the local and regional air quality.

Acknowledgements

This project was served throughout by the efforts of a team of dedicated people drawn from students and staff of the Geography Department, University of Guelph, Guelph, ON, and from members of Tsay Keh Dene. This work could not have been completed without their contributions of technical and labour support, often under somewhat trying environmental conditions, and intellectual contributions through data reduction, analyses, and reporting. The contributions of support from Dr. Vic Etyemezian and Mr. George Nikolich, DustQuant, Inc. are also gratefully acknowledged.

The Guelph team was comprised over the four years of the study by: Laura Brown, Janelle Trant, Dinyar Minocher, Mario Finoro, Sandy McLaren, Adam Bonnycastle, Jess Rogers, and Aaron Berg.

Tsay Keh Dene team members included: Cody Davis, Emma-Lena Lezard, and Luke Powell.

We would also like to thank all the people who contributed their support to keep us all well-fed at the Davis Camp (Roma Bird, Lena McCook, Violette Messenger, and others) and maintained contact with us as we moved about the reservoir creating a safer working environment (George and Vicki Podgorenko), and for the boat crew (Darren, Travis, and Marty) who transported the team and the PI-SWERL to various locations around the reservoir often unloading the gear in very creative ways. We also acknowledge the hospitality of Ft. Graham Lodge, where, on occasion, members of the team were billeted when Collins camp was full.

The support of Aaron Flett, Dean Daley, and Harry Brownlow (BC Hydro) in carrying out this project is also gratefully acknowledged.

1.0 INTRODUCTION

Each year the draw-down of the Williston Reservoir for the production of hydro electric power exposes several thousand hectares of wide flat beaches comprised predominantly of relatively fine grained sediments. These sediments are very prone to deflation by wind resulting in large dust storms that may affect human health and the quality of life for inhabitants of the valley.

Various control measures have been initiated at the reservoir, with the primary method being tillage. From 2009 through 2012 we have undertaken a measurement strategy to delineate the location and areal extent of those beaches that are most likely to erode at any given time. Knowledge of the likelihood of an erosion and dust emission event is desirable so that a given control method can be implemented at the right location in a timely manner to allow preventive measures to be undertaken to reduce or eliminate dust emissions. This approach can result in reduced control costs by applying appropriate mitigation measures to only those areas that have the greatest potential to erode and release dust. Although no predictive model of this nature currently exists, remote sensing and field techniques as well as modeling approaches are available that can be used to guide the development of an effective methodology and predictive wind erosion model for the Williston Reservoir.

1.1 STUDY GOALS AND OBJECTIVES

In 2009 a project was initiated with the goal to evaluate the feasibility of using RADARSAT-2 as a means to acquire data on the emission condition of Williston Reservoir beaches that could be used in the development of a dust emission model. Although good progress was made towards the development of the dust emission model, RADARSAT-2 was found to be too costly and difficult to manipulate for this particular application. As a result, a different approach using LANDSAT imagery was adopted. As part of this feasibility study, potential dust emissions, which provide necessary input for the model, were evaluated at selected beaches on the Williston Reservoir using the Portable In-Situ Wind Erosion Lab PI-SWERL) (Etyemezian et al., 2007). This instrument is being used increasingly as a primary tool to evaluate windblown dust emissions from natural and artificial soil surfaces because of its ease of operation and cost effectiveness when compared to larger, more logistically challenging, portable field wind tunnels (e.g., Bacon et al. 2011, Etyemezian et al. 2007, Kavouras et al. 2009, Sweeney et al. 2008, 2011, 213). Beginning in 2010 a more intensive measurement campaign was initiated to obtain additional data on the potential emission of particles less than or equal to 10 µm aerodynamic diameter (i.e., PM_{10}), for beaches that surround the Williston Reservoir using the PI-SWERL. In addition to the PI-SWERL measurements, data on the grain size of the beach sediments and their moisture content at the time of testing were collected. These two characteristics of the sediments can critically affect the wind speed needed to mobilize the sediments as well as the

strength of the dust emissions. In order to extend the range and general applicability of the dust prediction model, it was deemed necessary to carry out additional PI-SWERL testing on additional beaches as well as some of the same beaches tested in 2010, in spring 2011 and 2012.

The overall goal of the 2012 measurement campaign was to increase the available database that has been developed to characterize the spatial and temporal variability of dust emission potential for the Williston Reservoir beach environments. In addition data were collected that provide information on the temporal variability of the threshold wind speed at which dust emissions begin. These new data are used to better-define the relationships between these parameters and surface moisture content and textural conditions, and link these measurements to specific geographic locations. A knowledge of emission potential as a function of location can serve as a powerful guide for directing dust mitigation operations.

To achieve the above stated goal, two major objectives were developed for the 2010 field study and carried forward to the 2011 and 2012 studies:

1) Quantify the range of potential dust emissions at beaches throughout the reservoir to the best of our ability to meet the challenges of weather, travel restrictions, and other logistical constraints.

2) Identify the locations, textural characteristics, associated threshold wind speed and potential emissions from "hot spots" where a large percentage of the total atmospheric dust loading may originate.

3) In 2012 we also investigated the use of a Lagrangian Particle Dispersion Model to identify the relative contributions from different beaches that impact the air quality (i.e., PM_{10}) concentrations in Tsay Keh village under several different dust event conditions using wind data measured during storms that occurred during the tillage trials, emission fluxes measured for the different beaches from the PI-SWERL measurements, and ambient 24-hour PM_{10} data from the Partisol Sampler located on Tsay Keh beach at the time of the dust events.

2.0 Measuring Dust Entrainment Thresholds and Emission Fluxes

Critical parameters for evaluating the dust emission characteristics of a susceptible surface include the wind speed, or more correctly the wind shear stress (τ, N m^{-2}) or wind shear velocity (u_*, m s^{-1}, note $\tau = \rho \times u_*^2$ where ρ is air density, kg m^{-3}) that causes the sediments to be entrained into the wind (i.e., the threshold for entrainment), as well as the strength of those dust emissions (i.e., emission rate, F, µg m^{-2} s^{-1}) in relation to the magnitude of the shearing stress. Particle emission thresholds are critically controlled by: particle size of the sediments,

moisture content, soil texture (i.e., percent sand, silt, and clay), and surface roughness. It is generally accepted that the dust emission scales as power function of the wind shear stress (e.g., Shao 2000), with recent theoretical evaluations (e.g., Shao 2004) supporting a third power relationship (i.e., $F \propto a\ u_*^3$), but a wide range of exponent values have been observed (Gillies 2013).

2.1 Measurement Program

Following directly from the successful measurement campaign of 2009, 2010, and 2011 that used the PI-SWERL, this instrument was utilized again in 2012. The PI-SWERL is highly portable, operated by one to two people, and economical for field measurements with a typical test completed in less than 20 minutes. Direct comparisons of PI-SWERL measurements with the University of Guelph, straight-line field wind tunnel at seventeen sites in the Mojave Desert (Sweeney et al. 2008) showed very good correspondence between the two measurement methods.

2.2 Site Selection

In spring 2012, beaches for sampling were selected based on knowledge gained from the study of Nickling et al. (2011), as well as observations made by the field team in 2011, and in consultation with other personnel working at the reservoir who have traversed much of the reservoir beaches carrying out various activities (e.g., tilling operations, archeological work, project management, etc.).

The sampling locations were selected, as much as possible to capture the diversity of soil characteristics of the beaches surrounding the reservoir and their associated dust emission potential. A constraint on the sampling program was travel restrictions in that the beaches had to be accessible to all-terrain vehicles (i.e., a Ranger), which was especially relevant for the transportation of the PI-SWERL. PI-SWERL was transported to the beaches by a Ranger. A list of the test locations where PI-SWERL and surface characterization data were collected are presented in Table 2.1.

Table 2.1. The date, time, and location of the PI-SWERL transects carried out in 2012.

Date	Location	Transect	Time		Number of valid tests
			Beginning	End	
15-May-12	Collins	1	15:14	17:19	10
16-May-12	Collins	2	9:42	11:13	10
	Collins	3	11:44	13:02	5
17-May-12	DavisS	1	9:49	13:17	10
	DavisS	2	13:30	14:50	8
18-May-12	DavisS	3	9:20	10:56	10
25-May-12	Bob Fry S	1	12:27	13:56	10
	Bob Fry S	2	14:03	15:38	10
26-May-12	Tsay Keh	1	11:31	13:00	10
	Tsay Keh	2	13:14	14:40	10
27-May-12	Tsay Keh	3	13:07	14:34	10
28-May-12	Corless A	1	9:08	10:42	10
	Corless A	2	11:03	12:23	9
	Corless A	3	12:43	12:09	10
30-May-12	Corless B	1	8:44	10:11	10
	Corless B	2	10:17	11:49	10
	Corless B	3	11:59	13:23	10
8-Jun-12	Von Somer	1	15:24	16:07	5
	Von Somer	2	16:09	16:52	5
9-Jun-12	Von Somer	3	10:22	11:05	5
	Chowika	1	12:00	12:45	5
	Chowika	2	12:54	14:57	5
	Chowika	3	13:53	14:39	5
	DavisN	1	16:11	16:56	5
10-Jun-12	DavisN	2	10:04	10:51	5
	DavisN	3	11:05	11:55	5
	Lafferty	1	14:13	14:59	5
	Lafferty	2	15:03	15:53	5
	Lafferty	3	16:07	16:44	5
12-Jun-12	Ospika	1	9:46	10:31	5
	Ospika	2	10:40	11:27	5
	Ospika	3	11:42	12:29	5
13-Jun-12	Pete Toy	1	11:58	12:44	5
	Pete Toy	2	12:49	13:35	5
	Pete Toy	3	13:37	14:23	5
	Stromquist	1	15:16	16:08	5
	Stromquist	2	16:02	16:45	5
	Stromquist	3	16:47	17:28	5
14-Jun-12	Shovel	1	13:38	14:21	5
	Shovel	2	14:25	15:08	5
	Shovel	3	15:10	15:52	5

2.3 Sampling Site Characteristics

In 2012, 12 beach areas were visited for to acquire measurements of potential dust emissions using the PI-SWERL. Brief descriptions of the characteristics found at each test site are provided in Table 2.2 along with a photograph of the area in which the PI-SWERL tests were undertaken.

Table 2.2. Descriptions of the PI-SWERL test sites, 2012.

(A) Bob Fry South **56°14.124', 124°20.180'**

(no photo available)

(B) Chowika **56°44.629', 124°21.231'**

Fine sand in parts. High percentage of large pebbles present. Moist conditions apparent over large areas.

(no photo available)

(C) Collins **56°25.504', 124°24.742'**

Mostly fine sand, with some sections of finer silt. Very wet towards south section of beach (old marsh), lots of coarse woody debris. Tillage above last summer's waterline is still very well formed, that below the waterline is non-existent. Located on the east shore. Sandy to sandy loam texture, easy to access, extensive area, heterogeneous composition.

(D) Corless A

56°26.361', 124°30.316'

Fine clean sand, well-formed wind ripples present.

(E) Corless B

56°26.000', 124°30.014'

Silty-sand texture, high pebble content, well developed wind ripples present.

(F) Davis N 56°32.753', 124°30.918'

Located on the east shore, site of previous tillage and vegetation trial. The majority of this beach is Loamy sand, with some regions having a high silt and clay content. extensive area, site of tillage and vegetation trials.

(G) Davis S 56°31.325', 124°30.307'

Located on the east shore, accessible by road at Fort Graham. The majority is medium sand (especially around the middle of the beach), similar to Davis North. Lots of pebbles and coarse sand towards the north (above and below the waterline). Finer sediments towards the south.

(H) Lafferty **56°19.691', 124°29.212'**

Located on the east shore, south of Collins. Mostly fine sand, with some sections of finer silt. No evidence of last year's tilling. Significant coarse woody debris cover and very shallow water adjacent to beaches.

(I) Ospika **56°12.563', 124°08.865'**

Located on the east shore. Combination of sand and gravel with several regions of organic matter. Relatively high sediment transport threshold. Accessible by road. Low emissivity.

(J) Pete Toy **56°29.699', 124°33.262'**

Very sandy.

(K) Shovel **56°35.829', 124°25.298'**

Located on the east shore. Very homogeneous sand, similar in composition to Davis, Lafferty and Middle Creek N and S. Some isolated silt patches. Accessible by boat. High emissivity.

(L) Stromquist **56°34.036', 124°37.696'**

(M) Tsay Keh **56°52.935', 124°57.865'**

Northernmost beach composed primarily of sand. Accessible by road from the village of Tsay Keh. High emissivity. Fine sand, remains of last year's tillage and plantings can be seen. Concentrations of large pebbles and rocks.

(N) Van Somer **56°49.215', 124°51.699'**

Located on the east shore, south of Ruby Red. Gravelly sand and moist conditions.

2.4 PI-SWERL Test Results 2012

2.4.1 Sediment Texture of the Sampled Beach Areas

The textural characteristics of the sediment samples collected at each beach tested in 2009, 2010, and 2011 are shown in Table 2.3. The beach environments tested in both 2009 and 2010 were predominantly classified as sand (65%), 20% of the test beaches are classified as loamy sand, 10% are sandy loam, and 5% are silty clay loam. In 2011 the beaches tested with PI-SWERL were either sand (67% of tests) or loamy sand (33% of tests).

Table 2.3. The textural characteristics and soil type designations of the test areas from 2009, 2010, 2011, and 2012.

Location	Average % sand	Average % silt	Average % clay	Average soil class
2009 Field Season				
Collins 1	88.2	4.5	7.3	loamy sand
Collins 2	89.8	3.8	6.4	sand
Collins 3	95.3	1.8	2.9	sand
Davis	94.3	3.3	2.4	sand
2010 Field Season				
Bevel	85.8	7.8	6.4	loamy sand
Bob Fry	3.4	58.5	38.1	silty clay loam
Collins	72.4	20.6	6.9	sandy loam
Corless A	95.9	1.4	2.7	sand
Corless B	95.9	1.5	2.6	sand
Davis North	84.6	10.9	4.5	loamy sand
Davis South	91.4	4.9	3.7	sand
Lafferty	76.5	17.3	6.2	loamy sand
Middle Creek N	92.4	2.1	5.5	sand
Middle Creek S	94.8	1.2	4	sand
Ospika	95	1.4	3.6	sand
Pete Toy	95.4	1.3	3.3	sand
Raspberry	95.8	1.4	2.8	sand
Ruby Red	69.4	25.4	5.2	sandy loam
Shovel	92.4	3.3	4.3	sand
Tsay Keh	89	6.5	4.5	sand
2011 Field Season				
Collins	86.2	11.3	2.5	sand
Corless A	95.8	3.9	0.3	sand
Corless B	97.9	1.6	0.4	sand
Davis N	71.9	22.9	5.2	loamy sand
Davis S	96.1	2.7	1.3	sand
Lafferty	74.9	21.1	3.9	loamy sand
Middle Creek N	95.3	3.6	1	sand
Middle Creek S	95.8	3.1	1.1	sand

Ospika	97.2	2	0.8	sand
Shovel	82.7	15.6	1.7	loamy sand
Tsay Keh	83.2	15	1.8	loamy sand
Von Somer	97.9	1.6	0.6	sand
2012 Field Season				
Bob Fry	24.3	21.7	54.0	Clay
Chowika	77.5	2.6	19.9	Loamy Sand
Collins	95.8	4.1	0.1	Sand
Corless A	99.5	0.0	0.3	Sand
Corless B	98.5	0.9	0.2	Sand
Davis North	92.8	3.4	3.8	Sand
Davis South	68.8	9.1	22.1	Sandy Loam
Lafferty	96.3	1.7	2.0	Sand
Ospika	96.5	3.4	0.2	Sand
Pete Toy	95.8	1.3	1.6	Sand
Shovel	91.6	4.8	3.6	Sand
Stromquist	98.1	0.7	1.2	Sand
Tsay Keh	97.8	3.4	-1.2	Sand
Von Somer	95.5	2.4	2.1	Sand

Comparing the textural characteristics of sites that have been measured over the four years of the program indicates that individual sites do change from year to year as a result of deposition during inundation or through wind erosion processes. Two locations have been measured for all four years, Collins and Davis South. Of these two sites, Davis South had a relatively stable texture for 2009 to 2011 with the percent sand varying on average 3%, silt 1.5%, and clay 1.6%, among the three years. In 2012, however, there was a change in the texture with a substantial decrease (27.3%) in the sand component and a large increase in the clay (20.8%), which would suggest that the emission potential of this beach should have increased in 2012. Collins shows a much higher degree of change among the four years of measurements, with a steadily increasing sand fraction from 2010 through 2012, with a concomitant decrease in the silt and clay fractions, indicating a potential trend towards a decreasing dust emission potential. In both cases (Collins and Davis) the clay content is the most stable component during the first three years of measurement, but there are major shifts in the amount of mass in this fraction at both locations in 2012. These shifts in clay content percent suggest that there is significant dynamism in the textural character of beaches on an annual time frame, but a four year record

cannot reveal with great confidence the range over which beach textures can change, nor can it be determined from these data what process or processes drive the changes. It does need to be noted that the clay fraction contains the PM_{10} and $PM_{2.5}$ and small changes in clay content likely have a large effect on emission potential.

There are six additional sites to compare textural changes between 2010 and 2012. The change in the mass fractions of sand and clay between years for the same site indicates large changes are possible in the clay content ranging in absolute value terms up to 100% (Fig. 2.1). For the period from 2010 through 2012 there appears to have been a general decline in the clay fraction for five of these six beaches, with only Shovel beach showing a decrease in 2011 followed by an increase in 2012. The change in the sand component between years ranges from near zero (0.1%) to 18% (Fig. 2.1), with some beaches showing a stable sand fraction, while others show a much greater variability. It should be noted that the percent change values are more dramatic for the silt and clay components because of the delta change in much smaller values than the sand component. Nevertheless, these data indicate that the sediment texture of a beach does vary in over space and through time and cannot be treated as being static and unchanging. These data remain limited to three years and the differences may be more reflective of spatial variation than temporal variation as the points of measurement are not exactly the same from year to year. A longer period of measurements of soil texture would be required to evaluate the temporal variability of this soil property and as noted above the mechanism that may cause these changes, assuming that temporal variability is being exhibited at these sites(as it was for measurements at the same locations), remains unknown. We suggest that the temporal variability in beach texture is driven, in part, by the suspended sediment concentrations of the contributing rivers in the spring runoff and the sedimentation patterns driven by the currents in the reservoir before and after ice is formed in the fall/winter periods.

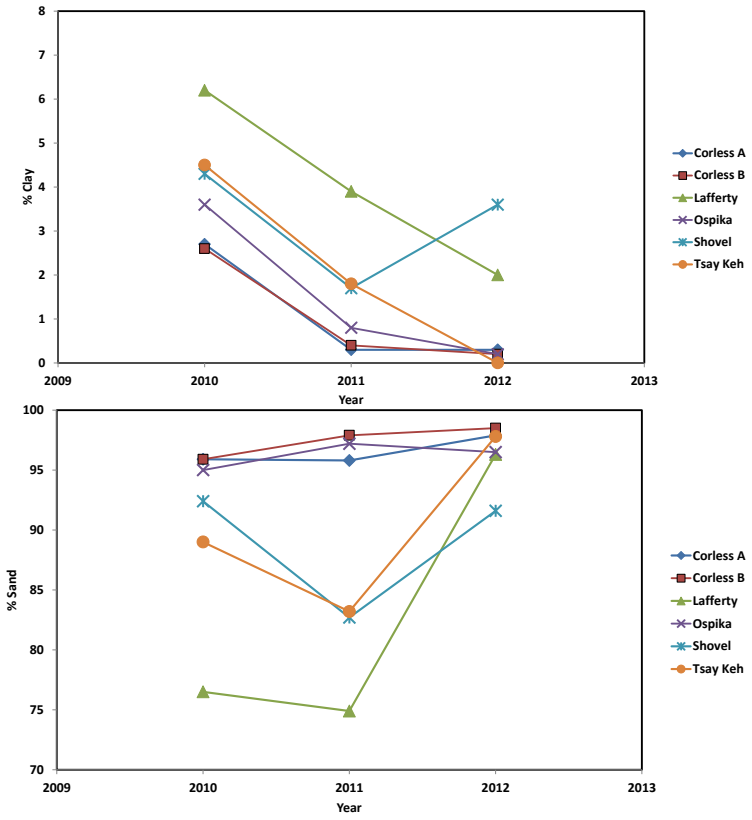

Figure 2.1. Annual changes in the clay and sand content of six beaches for the period 2010-2012.

2.4.2 Particle Thresholds for Sand and Dust Entrainment

Entrainment threshold for the sand-sized particles and the emission of PM_{10} dust were determined from the particle count and PM_{10} concentration data obtained during the initial ramp period when the PI-SWERL blade accelerates from 0 to 1000 RPM. To define when (and at what magnitude of shear stress) transport begins we followed the same criteria used by Nickling et al. (2010 and 2011). Due to instrument malfunction (OGS sensor) there are no data for particle threshold for: Ospika, Pete Toy, Stromquist, and Shovel beaches in 2012.

The observed threshold shear velocity (u_{*t} m s^{-1}) values for sand movement (saltation) were, in general, higher than those calculated for previous years (Table 2.4). In 2012 the minimum particle threshold was of 0.28 m s^{-1} for Davis N, with a maximum of 0.47 m s^{-1} measured for Davis N., Bob Fry, and Corless B. The lowest threshold shear velocity (u_{*t} m s^{-1}) values for PM_{10} dust emissions in 2012 (Table 2.4) was Van Somer (0.18 m s^{-1}). For comparison, the lowest mean u_{*t} in 2011 was Davis N and Van Somer (0.17 m s^{-1}). The beach with the highest u_{*t} for PM_{10} dust in 2012 was Bob Fry S (0.46 m s^{-1}).

Table 2.4. Threshold shear velocity (u_{*t}) statistics for sand on the tested beaches in 2012.

Location	# of tests	u_{*t} (m s^{-1}) Min.	u_{*t} (m s^{-1}) Max.	u_{*t} (m s^{-1}) Mean	Std. Dev. (m s^{-1})
Collins	18	0.38	0.46	0.42	0.02
Davis N	12	0.28	0.47	0.43	0.07
Davis S	15	0.41	0.46	0.45	0.01
Bob Fry S.	7	0.45	0.47	0.46	0.01
Shovel	N/A	N/A	N/A	N/A	N/A
Corless A	12	0.31	0.45	0.38	0.04
Corless B	19	0.37	0.47	0.42	0.03
Tsay Keh	27	0.37	0.46	0.43	0.03
Lafferty	9	0.35	0.46	0.44	0.04
Von Somer	14	0.38	0.46	0.45	0.02
Ospika	N/A	N/A	N/A	N/A	N/A
Chowika	16	0.36	0.46	0.44	0.03
Stromquist	N/A	N/A	N/A	N/A	N/A
Pete Toy	N/A	N/A	N/A	N/A	N/A

Using all the available u_{*t} data, the mean and standard deviation for each beach tested for all tests are shown in Tables 2.4 (sand) and 2.5 (dust). Corless A beach has the lowest mean u_{*t} value for sand (0.38 m s^{-1} m s^{-1}) and Bob Fry S the highest mean u_{*t} (0.46 m s^{-1}). The beach with the lowest mean u_{*t} for PM_{10} dust emissions in 2012 was Shovel (0.27 m s^{-1}), for comparison the lowest mean u_{*t} in 2011 was Davis N and Van Somer (0.17 m s^{-1}). The beach with the highest mean u_{*t} for PM_{10} dust was Chowika (0.39 m s^{-1}). . These threshold shear velocities are typical of those reported in the literature for sandy to sandy loam soils. The range of u_{*t} measured for sand movement (0.38 to 0.46 m s^{-1}) would be associated with 10 m wind speeds of 11.7 to 14.2 m s^{-1} (≈42 km $hr^{-1}$to ≈51 km hr^{-1}) assuming an average aerodynamic roughness length derived from the meteorological tower vertical wind speed profiles measured on Davis beach in 2010.

As Figs. 2.2 and 2.3 show there is year to year variation in u_{*t} at the same locations. Until 2012 there was more variability in the dust emission threshold than the sand threshold, but this does not hold with the inclusion of the 2012 data. Overall the dust threshold is less variable over the three years of measurement than the sand threshold, but for the sand threshold this is due entirely to the 2012 data. For all the beaches tested in 2010, 2011, and 2012 the measured mean values of u_{*t} for sand are the highest in 2012. The average percent increase in u_{*t} values between the 2011 and 2012 is 66% (±30%). The change in the dust emission threshold between 2011 and 2012 is small, 4.5% (±9%) and includes both positive and negative changes across the eight sites measured in both years. The changes in sand threshold values were all positive increases.

Table 2.5. Threshold shear velocity (u_{*t}) statistics for dust on the tested beaches in 2012.

Location	# of tests	u_{*t} (m s^{-1}) Min.	u_{*t} (m s^{-1}) Max.	u_{*t} (m s^{-1}) Mean	Std. Dev. (m s^{-1})
Collins	24	0.21	0.39	0.30	0.05
Davis N	12	0.25	0.36	0.28	0.03
Davis S	28	0.20	0.40	0.29	0.05
Bob Fry S.	16	0.32	0.46	0.37	0.04
Shovel	15	0.20	0.34	0.27	0.03
Corless A	29	0.27	0.31	0.30	0.01
Corless B	29	0.21	0.39	0.30	0.04
Tsay Keh	30	0.25	0.42	0.32	0.06
Lafferty	15	0.32	0.44	0.37	0.03
Van Somer	15	0.18	0.40	0.34	0.05
Ospika	13	0.28	0.42	0.37	0.05
Chowika	17	0.31	0.46	0.39	0.05
Stromquist	15	0.19	0.31	0.28	0.03
Pete Toy	15	0.25	0.32	0.28	0.02

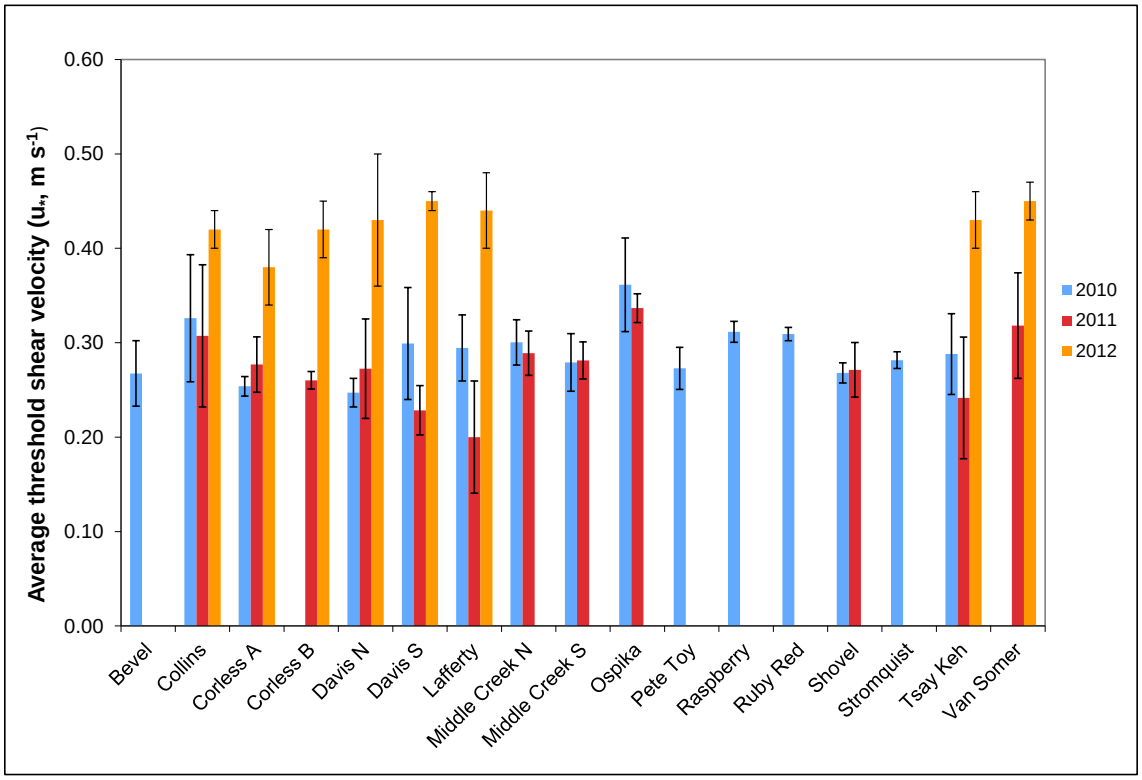

Figure 2.2. The mean threshold shear velocity (u_{*t}, m s^{-1}) for sand for each test site for all valid tests in 2010, 2011, and 2012. Error bars represent the standard deviation of the mean.

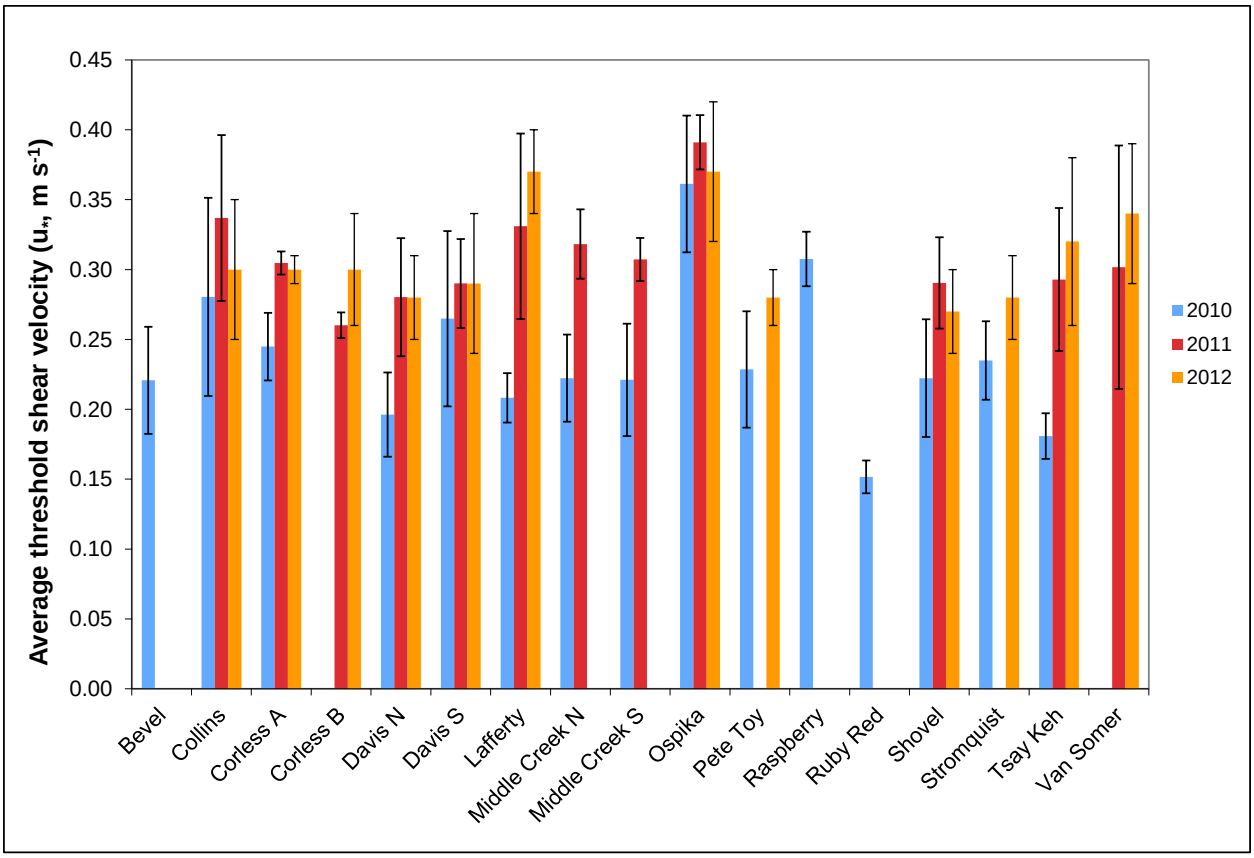

Figure 2.3. The mean threshold shear velocity (u_{*t}, m s^{-1}) for PM_{10} for each test site for all valid tests in 2010, 2011, and 2012. Error bars represent the standard deviation of the mean.

2.4.3 Emissions of PM_{10} Mineral Dust from the Test Beach Areas

The dust flux, which is the amount of PM_{10} produced per unit area per second from a PI-SWERL test is determined from the measurement of the PM_{10} concentrations (C, µg m^{-3}) and the air flow (V, m^3 s^{-1}) through the instrument, and the known dimensions of the PI-SWERL annular blade (m^2). An emission flux (F, µg m^{-2} s^{-1}) can be calculated as:

$$F_{i,cum} = \frac{\sum_{begin,i}^{end,i} C \times V}{A_{eff}(t_{end,i} - t_{begin,i})} \quad (2.1)$$

where the summation occurs over every 1 s measurement during level i, beginning at $t_{begin,i}$ and ending at $t_{end,i,}$ with t as integer seconds. The measured dust concentration and flow rate are converted to an emission flux by the effective area of the PI-SWERL, A_{eff}, which is 0.026 m^2. The PI-SWERL tests measure the potential PM_{10} dust emissions from the surface at different equivalent wind shear velocities (i.e., u_*, m s^{-1}). The tests are conducted at pre-set equivalent shear velocities that can span the range 0.1 to 1.2 m s^{-1}. The corresponding wind speed for a u_* of 1.2 m s^{-1} is approximately 90 km hr^{-1} at 2 m above the ground, which would be an extreme

wind event. The range used for testing at the reservoir beaches is u_*=0.15 m s^{-1} to 0.46 m s^{-1}, which was determined based on testing to maximize the range but limit the concentrations of PM_{10} to values that did not over-range the instrumentation measuring mass concentration (i.e., PM_{10}) and saltation counts. The complete range of emission potential for the beaches measured in 2012 is shown in Fig. 2.4, and is similar to that observed for 2011 (Fig. 2.5). Compared to the range of emissions measured in 2010, however, 2010 had six beaches (Ruby Red, Tsay Keh, Davis North, Shovel, and Middle Creek North) with considerably higher emission potential at the highest applied shear velocity (Fig. 2.6).

A comparison of emission relationships estimated for beaches with a four year record (i.e., Collins, Davis South and Davis North [note 2009 Davis North consisted of one transect]) are shown in Figs. 2.7 – 2.9. The figures show there is considerable variability in the dust emission potential for the highest applied wind shear velocity (≈0.46 m s^{-1}) across the four years of observations. This variability is most pronounced for Davis N, >3000 µg m^{-2} s^{-1} for the highest applied shear velocity between 2010 and 2011. For Collins beach the maximum difference between years 2010 and 2011 is 1679 µg m^{-2} s^{-1} while for Davis S the maximum difference between 2010 and 2011 is 1034 µg m^{-2} s^{-1}. These data suggest that Davis beach, at least for the four available years of data is more variable than Collins beach.

This range of variability in the dust emission data is not exhibited by all beaches as revealed by the available data record for the other beaches. Beaches that have shown quite consistent emission potential relationships from year to year include: Corless A (Fig. 2.10), Ospika (Fig. 2.11), Pete Toy (Fig. 2.12), and Shovel (Fig. 2.13). Beaches that show variability in emission potential similar to that observed for Collins and Davis include: Tsay Keh (Fig. 2.14), Corless B (Fig. 2.15), and Lafferty (Fig. 2.16). With only one year's data available for Bob Fry South (Fig. 2.17) and Chowika (Fig. 2.18) it is not possible to comment on their potential year-to-year variability. The two years of data for Van Somer (Fig. 2.19) and Stromquist (Fig. 2.20) show a modest amount of variability in emission potential, but the pattern cannot be said to definitive based on just two years of data.

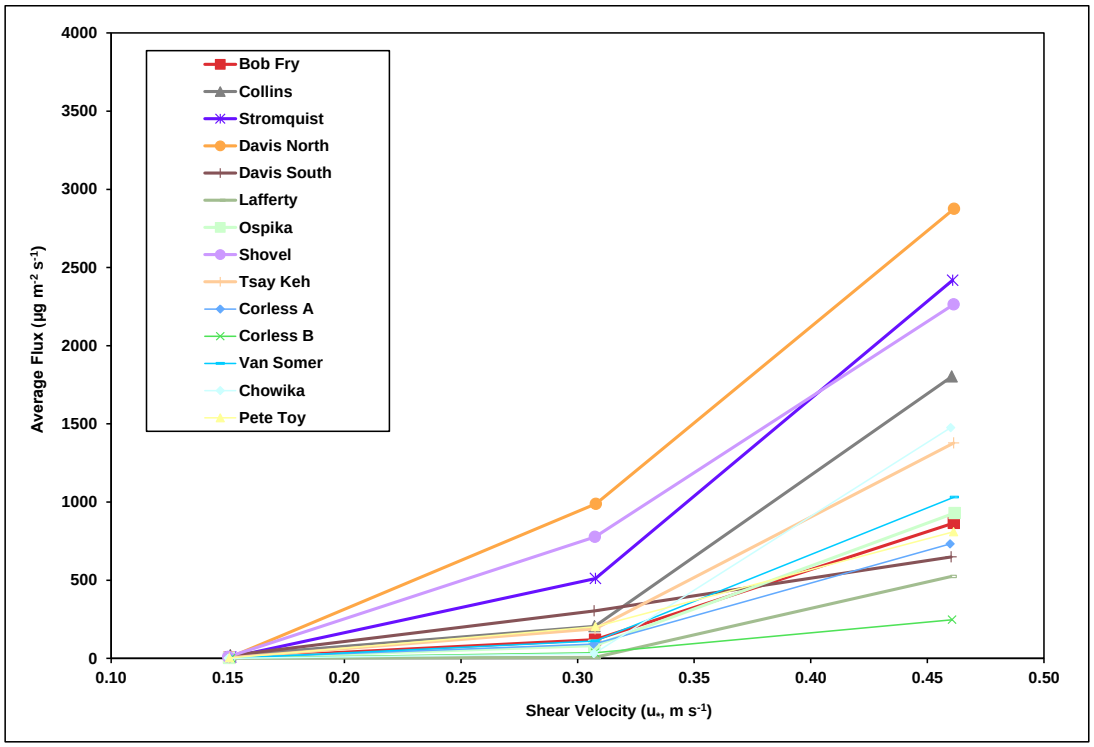

Figure 2.4. The average emission flux as a function of u_* for all of the test locations in 2012.

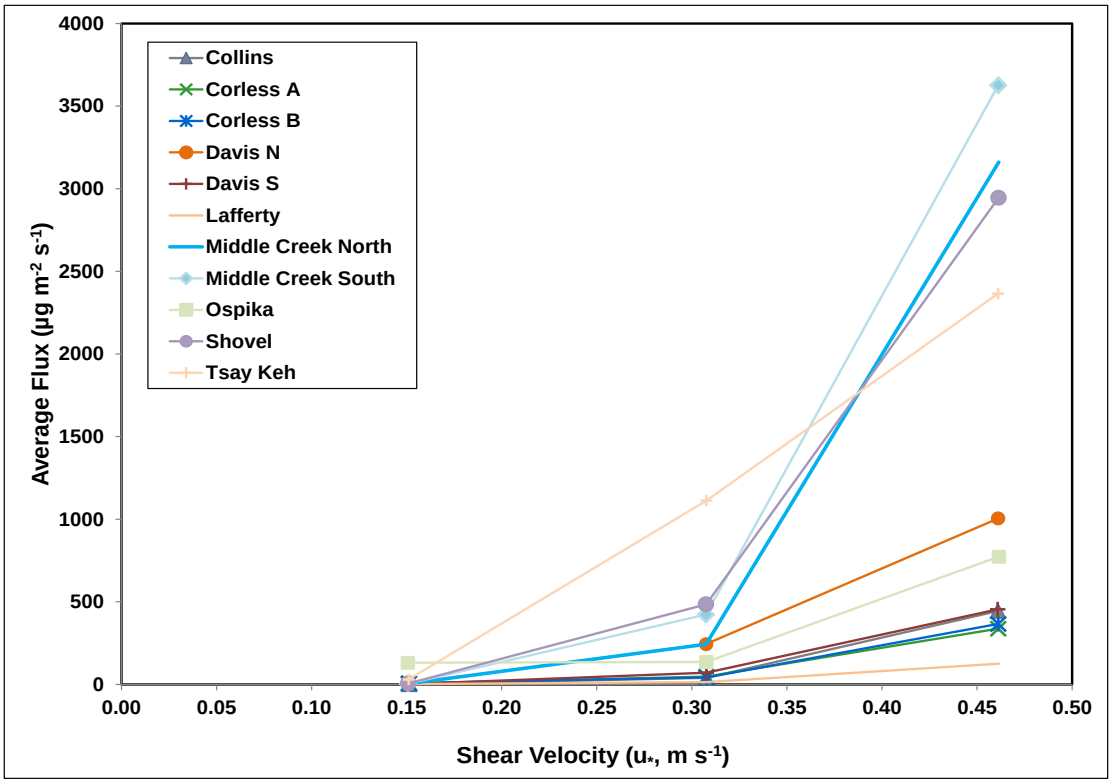

Figure 2.5. The average emission flux as a function of u_* for all of the test locations in 2011.

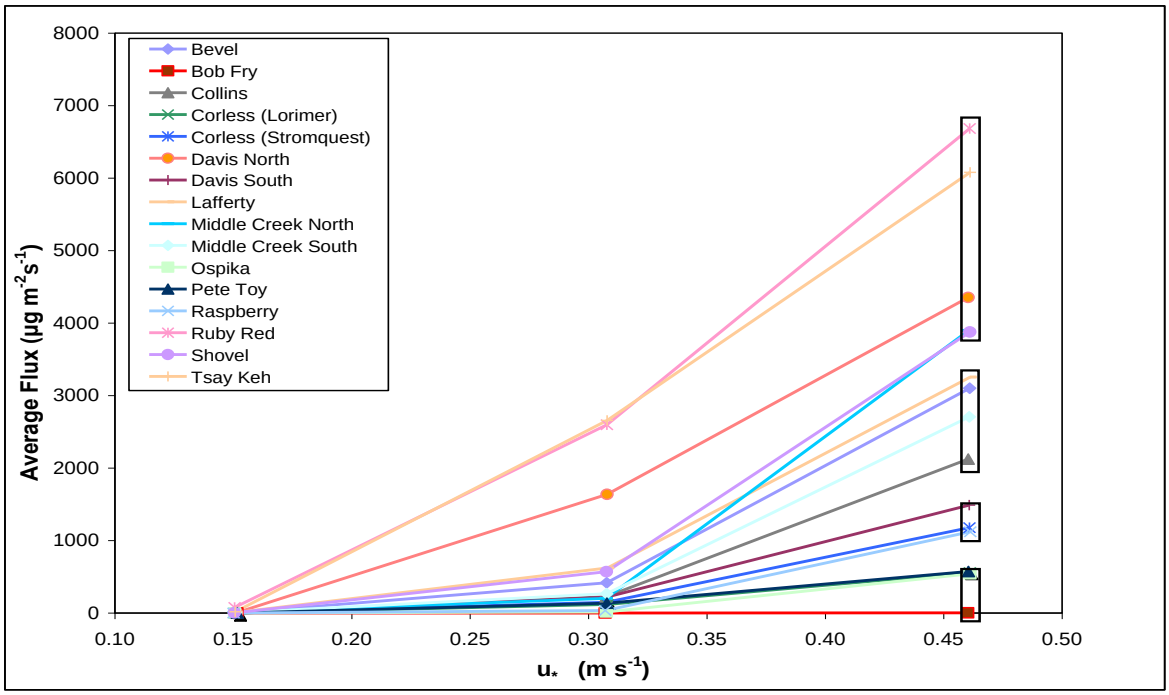

Figure 2.6. The average emission flux as a function of u_* for all of the test locations in 2010.

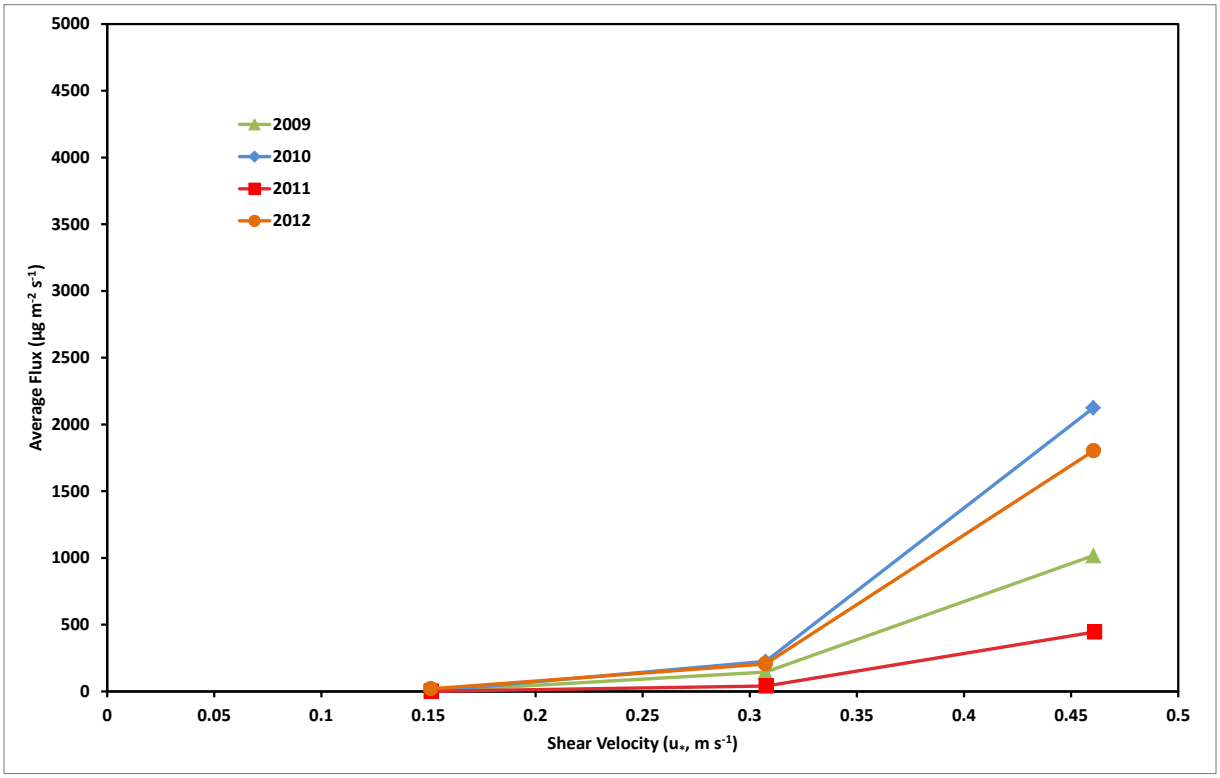

Figure 2.7. The emission relationships for Collins Beach 2009, 2010, 2011, and 2012.

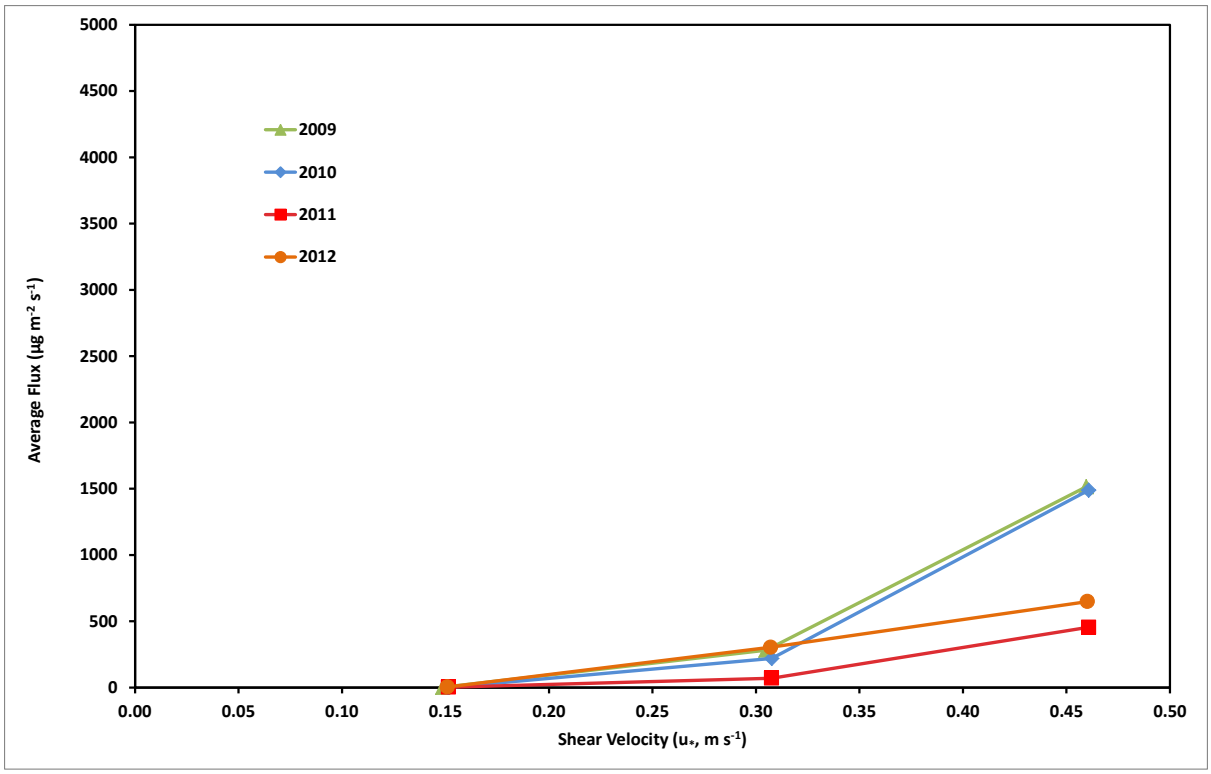

Figure 2.8. The emission relationships for Davis South Beach 2009, 2010, 2011, and 2012.

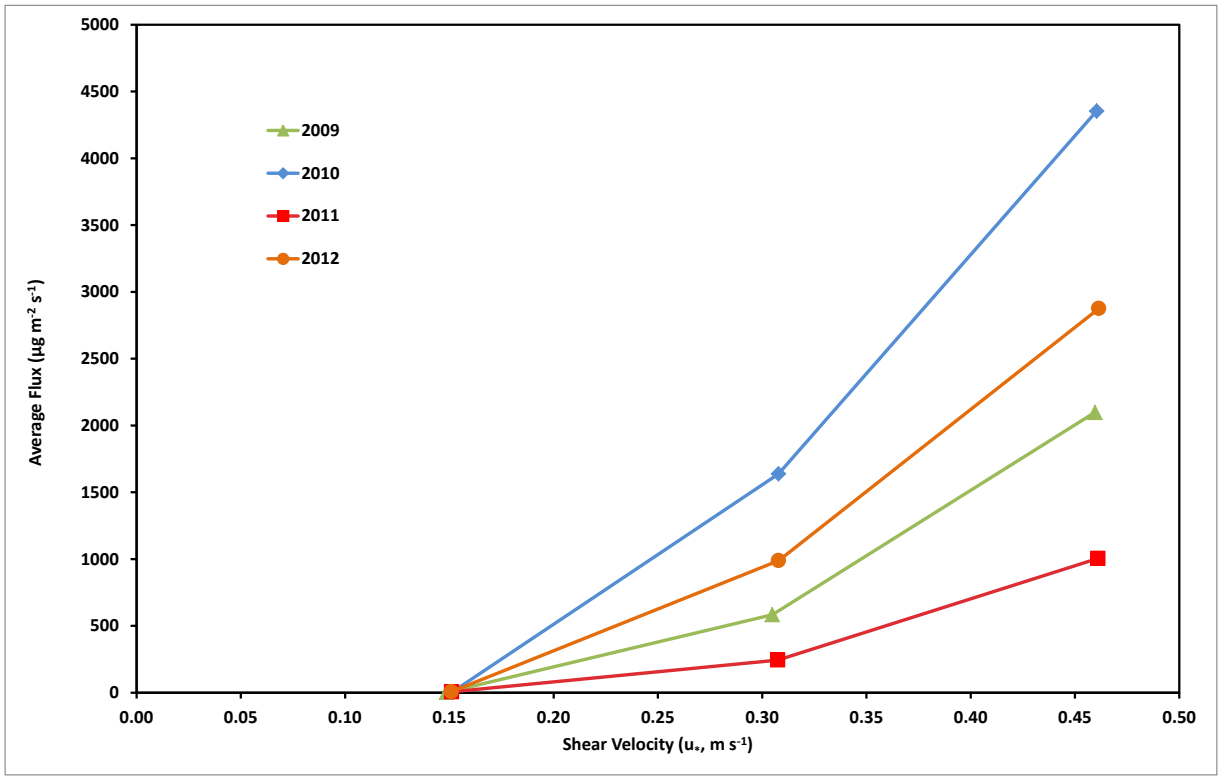

Figure 2.9. The emission relationships for Davis North Beach 2009, 2010, 2011, and 2012.

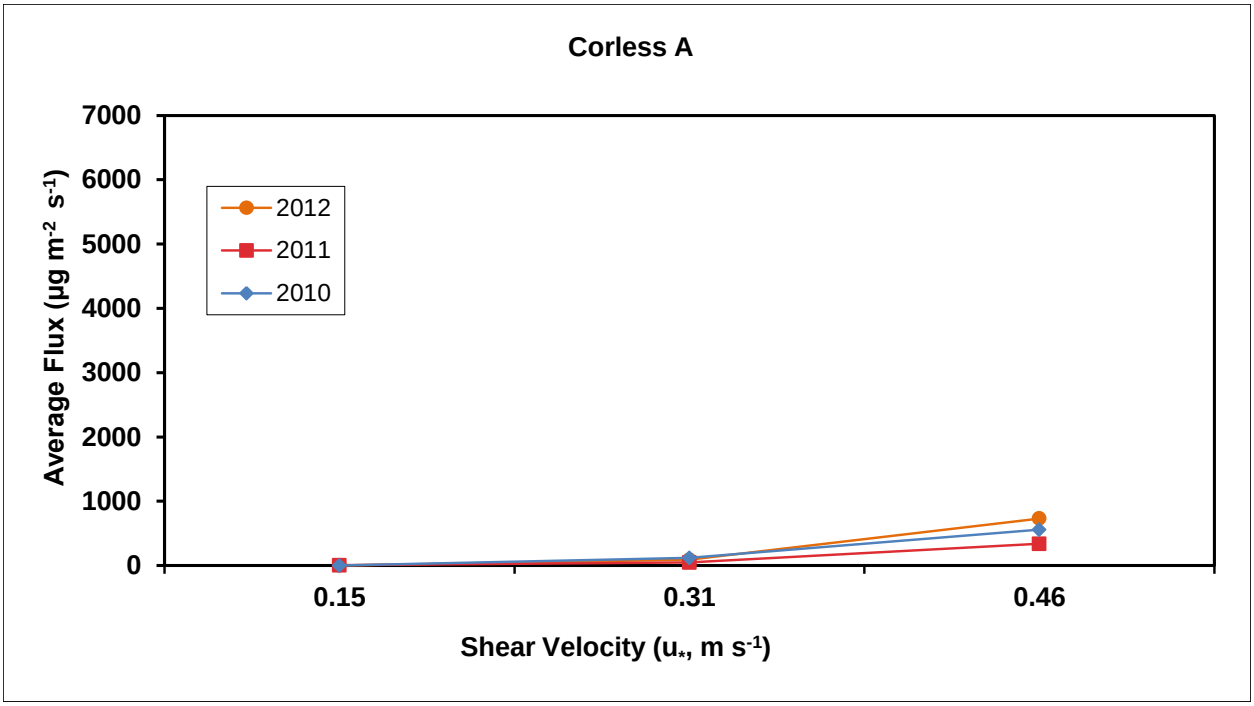

Figure 2.10. The emission relationships for Corless A Beach 2010, 2011, and 2012.

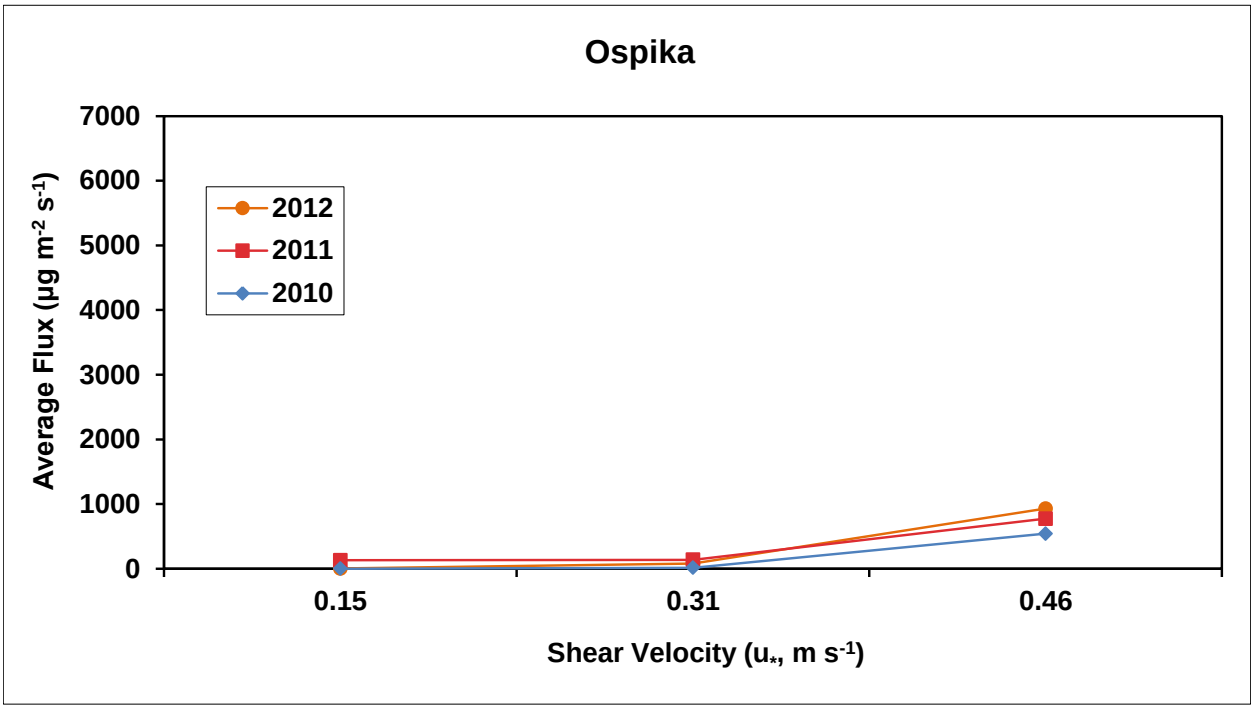

Figure 2.11. The emission relationships for Ospika Beach 2010, 2011, and 2012.

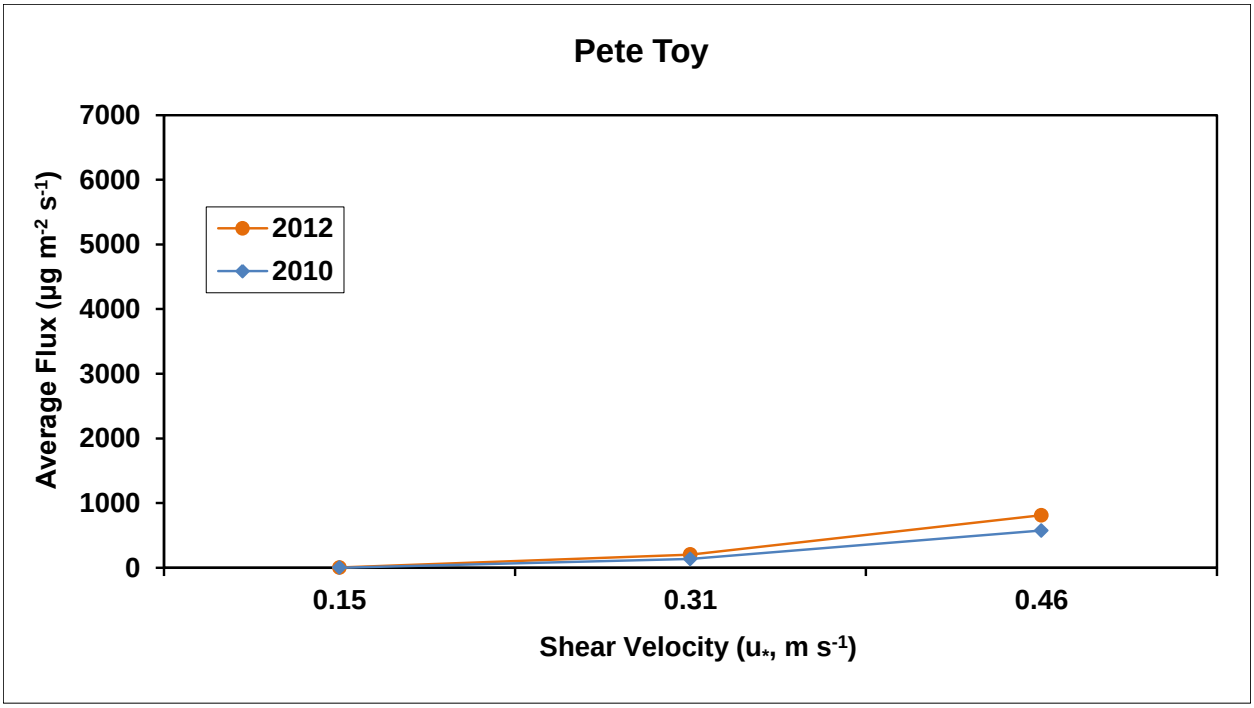

Figure 2.12. The emission relationships for Pete Toy Beach 2010 and 2012.

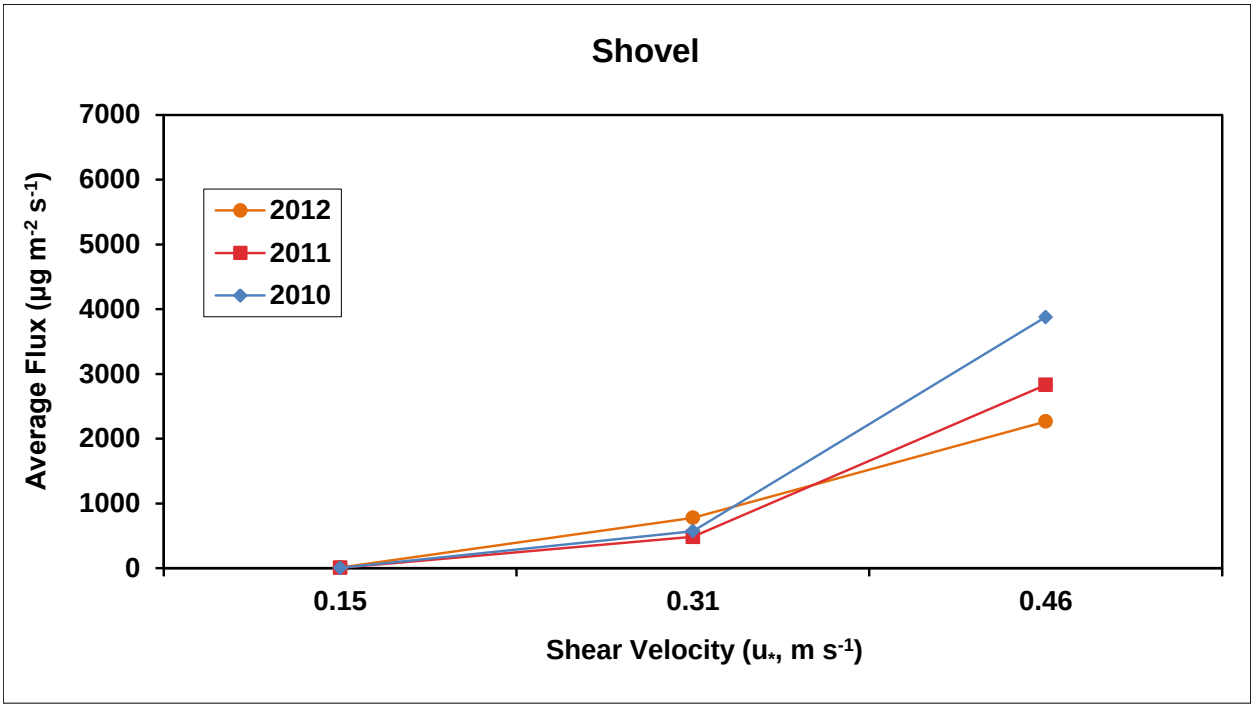

Figure 2.13. The emission relationships for Shovel Beach 2010, 2011, and 2012.

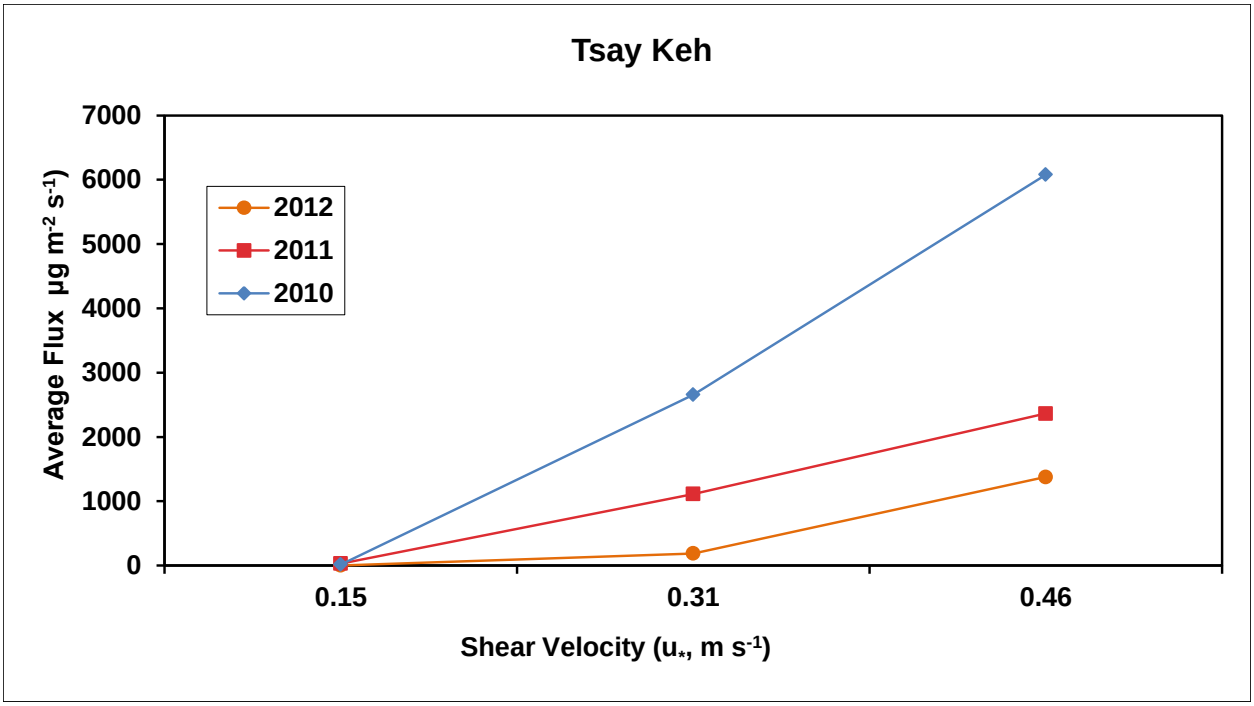

Figure 2.14. The emission relationships for Tsay Keh Beach 2010, 2011, and 2012.

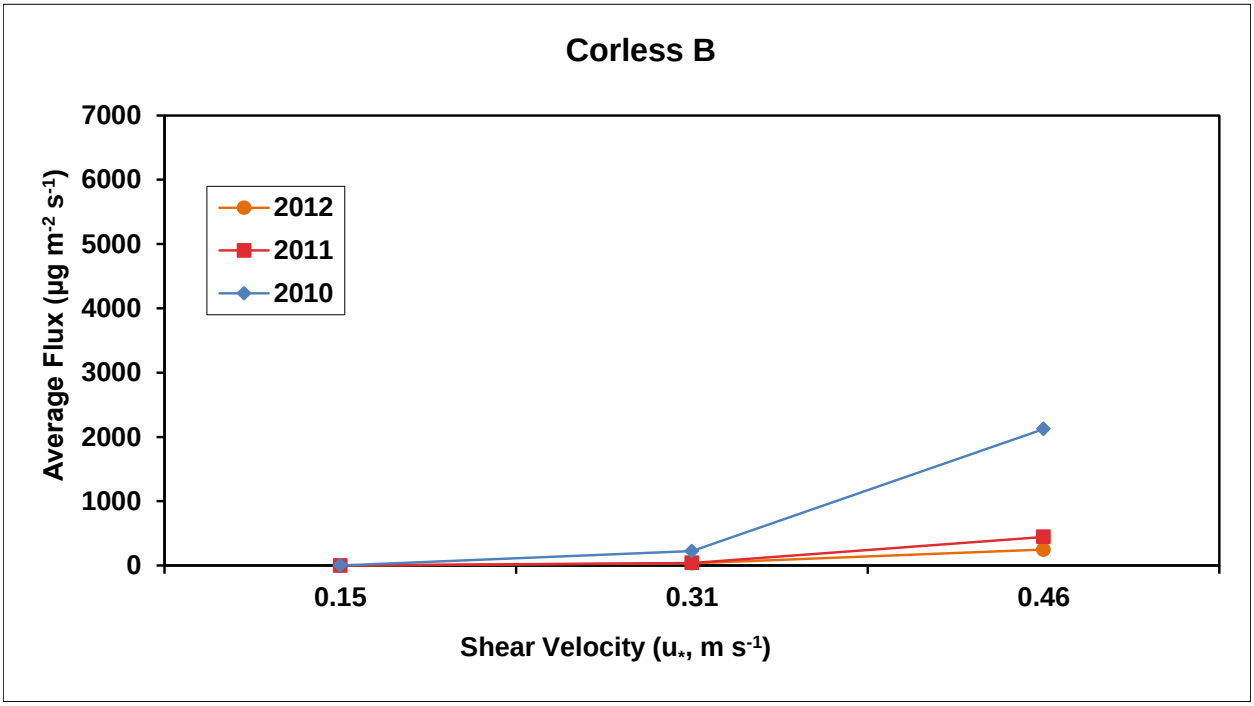

Figure 2.15. The emission relationships for Coreless B Beach 2010, 2011, and 2012.

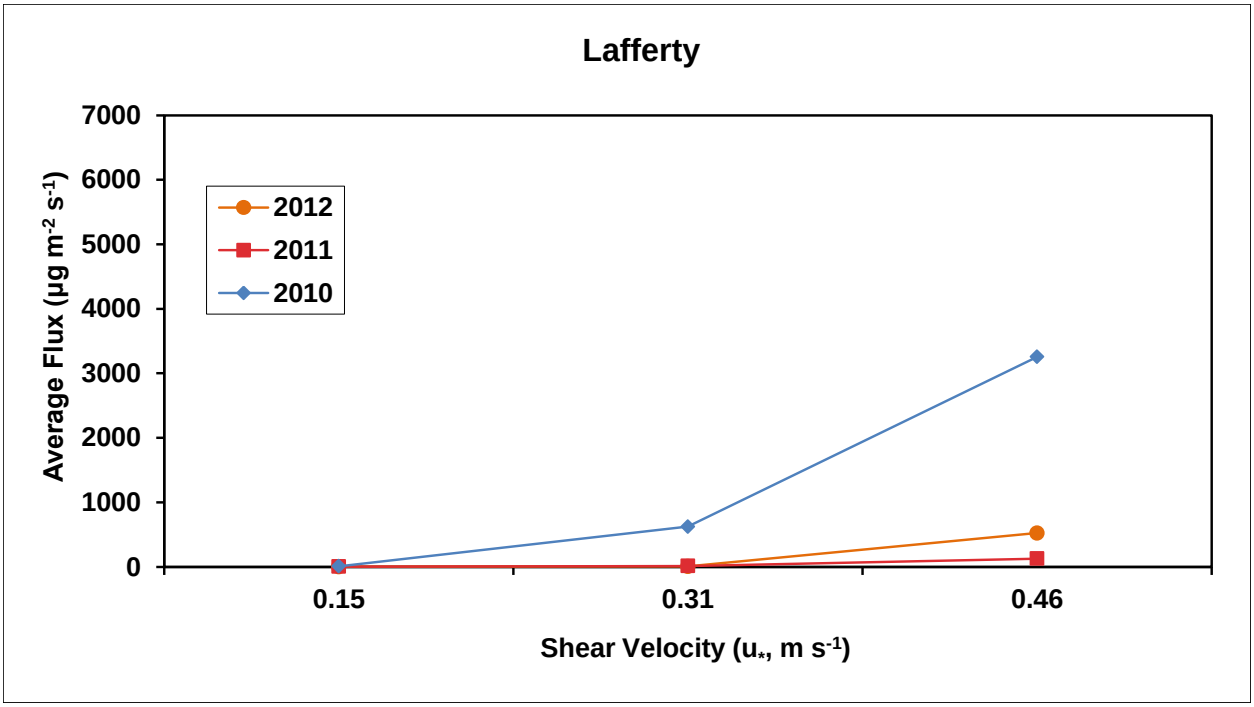

Figure 2.16. The emission relationships for Lafferty Beach 2010, 2011, and 2012.

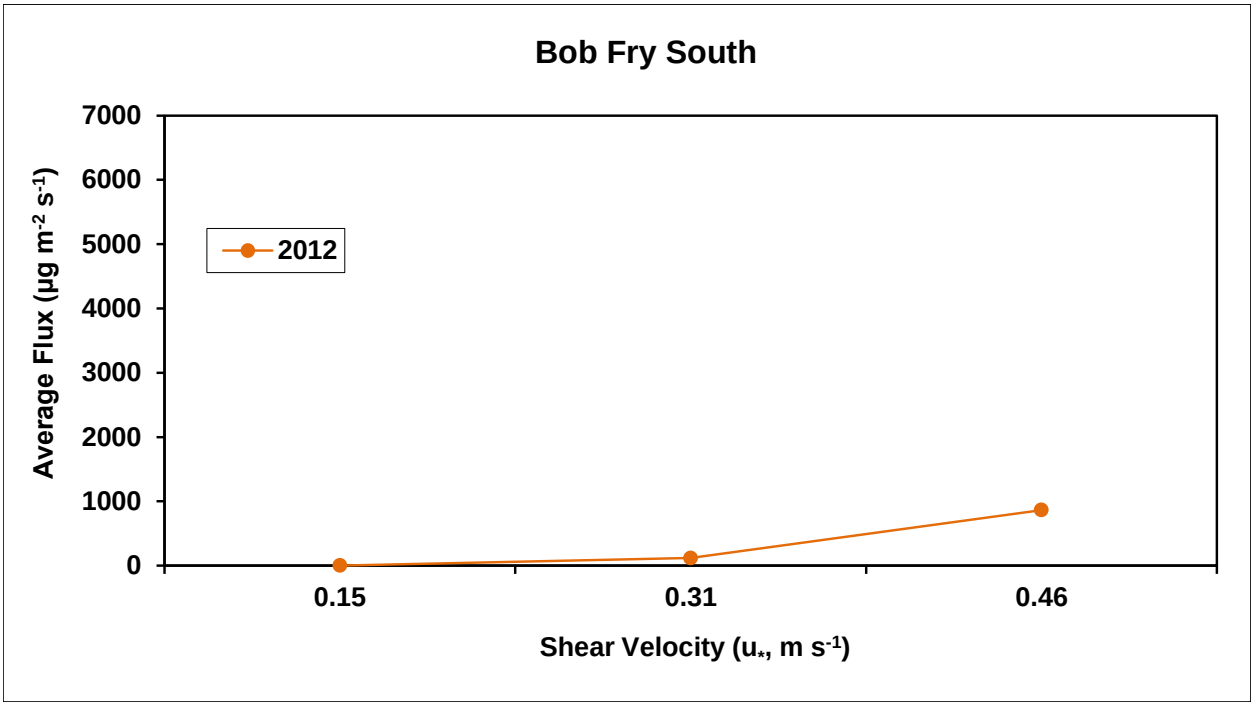

Figure 2.17. The emission relationship for Bob Fry South 2012.

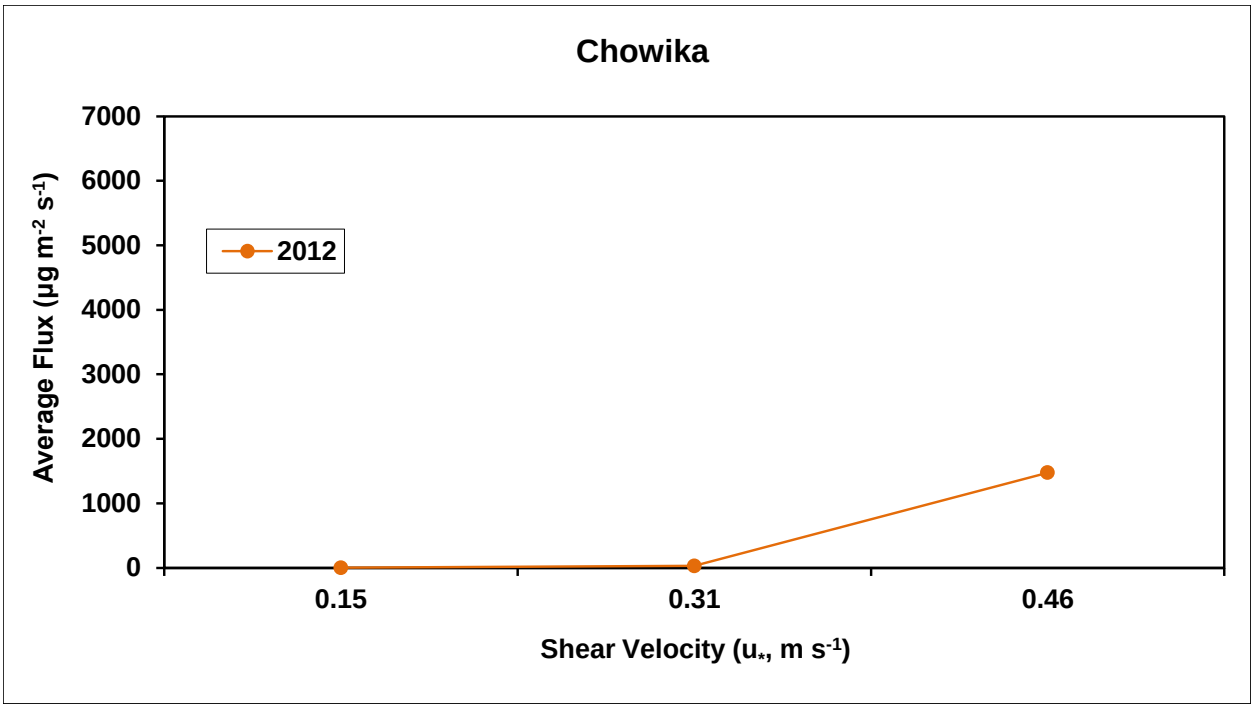

Figure 2.18. The emission relationships for Chowika Beach 2012.

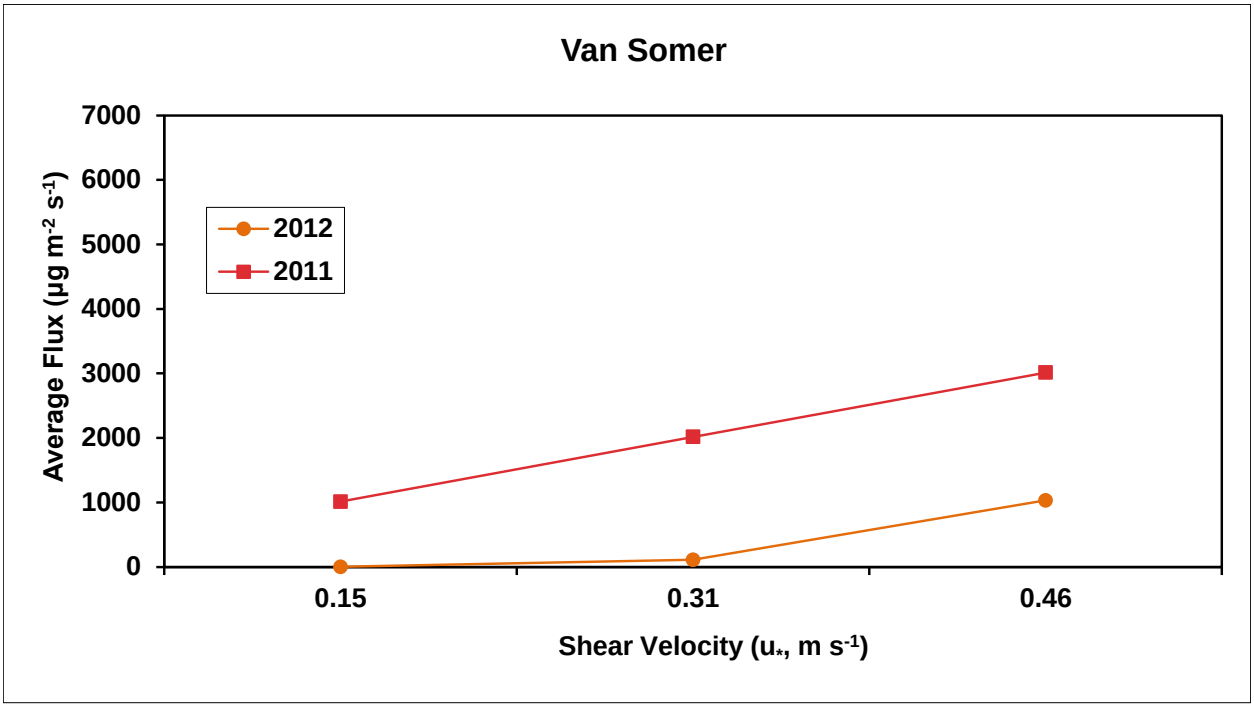

Figure 2.19. The emission relationships for Van Somer Beach 2011 and 2012.

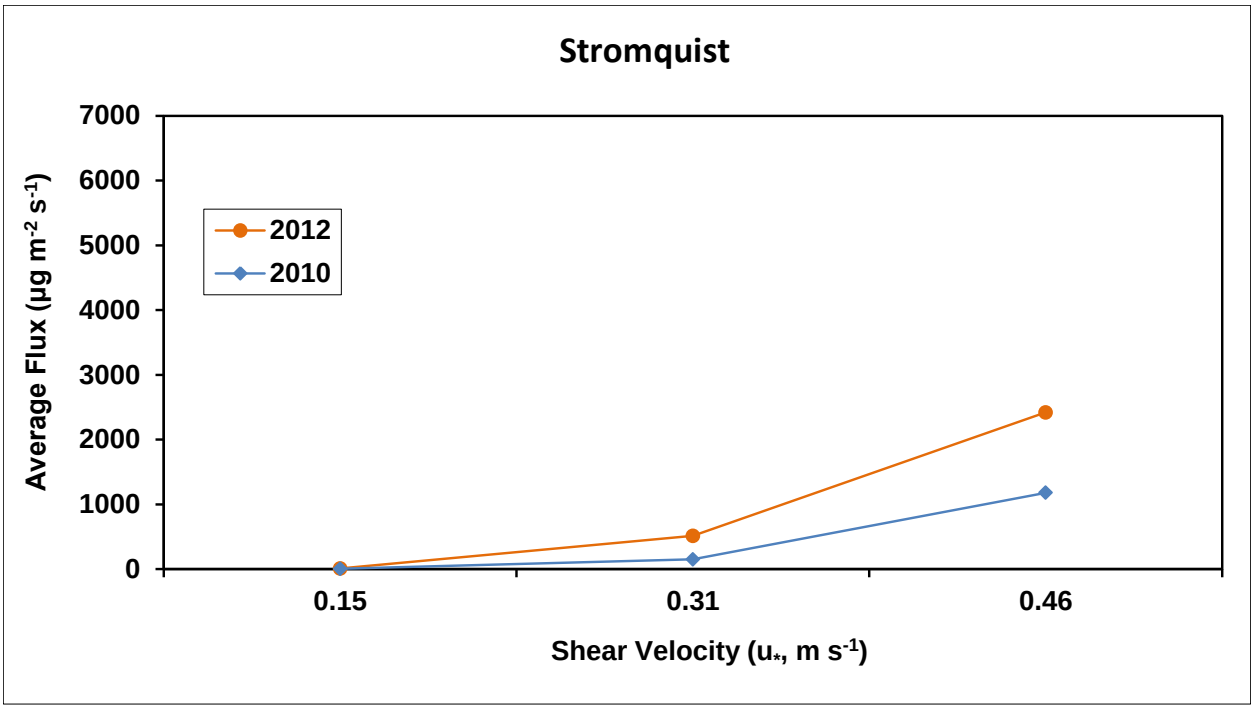

Figure 2.20. The emission relationships for Stromquist Beach 2010 and 2012.

Several reasons can be put forward to explain the variability or lack of variability in the emission potential of the beaches over space and through time. The first reason may be that because we did not measure at exactly the same locations for Collins and Davis beaches the year-to-year variability has been introduced by the sampling procedure. There is strong evidence however, that emission potential varies as a function of position on an individual beach as evidenced by the standard deviation of emission for a set shear velocity when multiple tests along multiple transects are examined. This variability in emissions, as a function of position, is shown by way of examples for Tsay Keh Beach (Fig. 2.21) and Shovel Beach (Fig. 2.21) in 2010 and 2012, respectively. The error bars on the data points represent the standard deviation of the mean around that value. The standard deviation of the mean shear velocity is typically around 1%, so it cannot be the source of the variation in the measured emissions.

A second reason for variability in the emission potential could be a function of the amount of suspended sediment, specifically in the clay fraction, which deposits onto the surface from the overlying water column when the reservoir full and during the subsequent drawdown of the water level. The amount of clay deposited to the surface is dependent upon several conditions including: 1) the spring melt, i.e., the volume of water entering the reservoir, 2) the amount of sediment within the water, 3) the distribution of the suspended sediment around the reservoir by the currents within the reservoir, and 4) the depositional environment that develops for

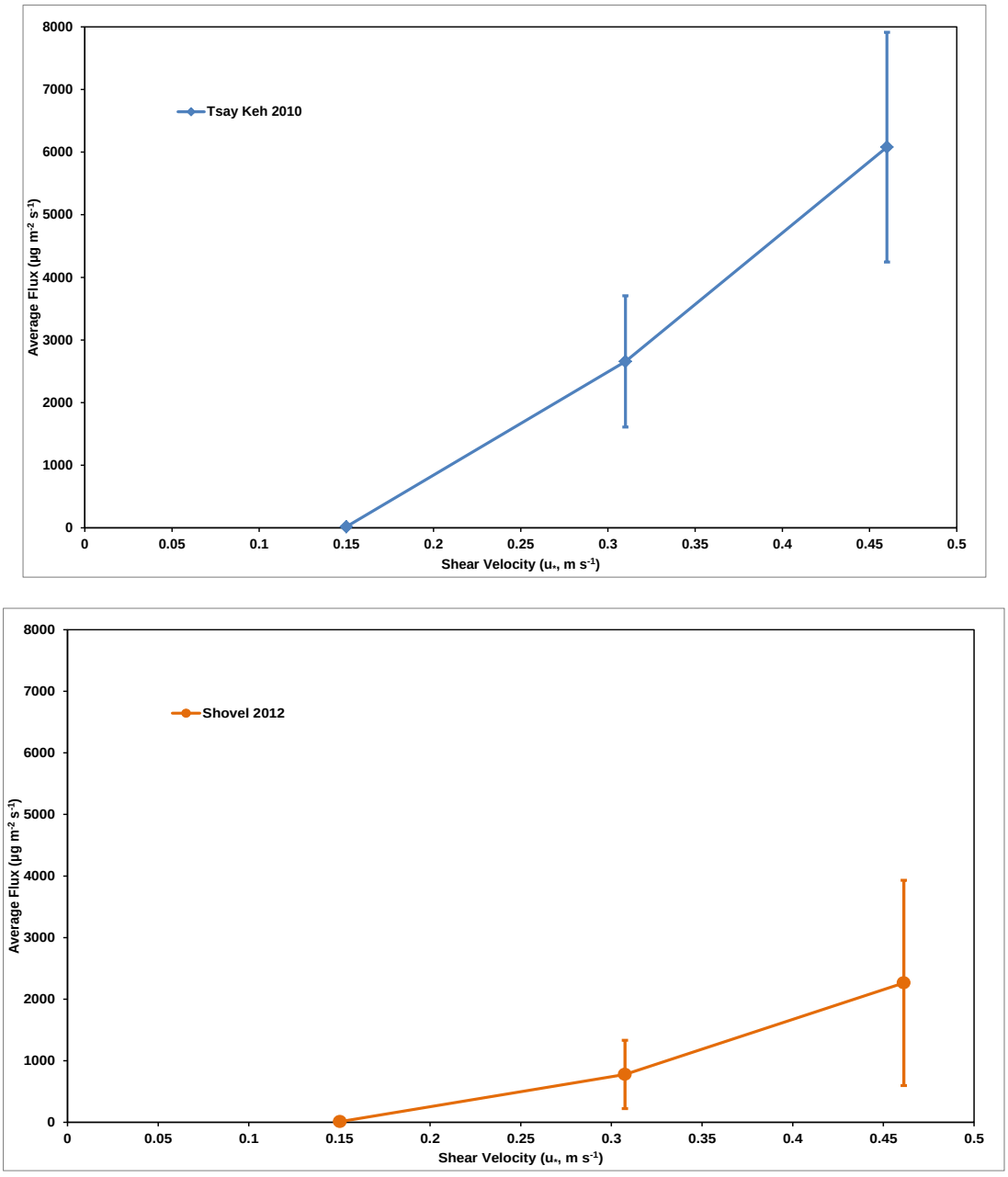

Figure 2.21. The emission relationship for Tsay Keh Beach 2010 (Top Panel) and Shovel Beach 2012 (Bottom Panel) showing the standard deviation about the mean value for a set shear velocity indicating variability in emission potential is a function of position on a beach.

each beach through the yearly cycle of open to ice-covered conditions. Potentially small changes in the silt and clay content of the sand of the beaches could translate into large changes in dust emission potential. The clay component represents the important reservoir for the PM_{10} dust that can be emitted from the surface under the action of wind and saltating sand. The linkages between the suspended sediments in the reservoir waters and the emission potential of the beaches remain to be established.

The four years of emission potential measurements obtained with the PI-SWERL indicate that, even taking the observed variability into account, there are beaches that have a consistently higher emission potential than others. Beaches that have the highest emissions >1500 μg m^{-2} s^{-1} at the highest applied shear velocity were: Shovel (2010-2012), Tsay Key (2010-2011), Davis N (2010, 2012), Middle Creek N (2010-2011), Middle Creek S (2010-2011), and Collins (2010, 2012). Other high emitting beaches, applying the same criterion, for one year of measurements were: Ruby Red, Lafferty, Bevel, Davis S, Stromquist and Chowika. These data suggest that due consideration be given to prioritizing mitigation treatments to those beaches listed in the first grouping. In addition, due to the proximity of Tsay Keh village to the potentially high emitting Tsay Keh beach it is suggested that this beach always be afforded a high priority for application of dust mitigation methods.

3.0 DUST EMISSION MODELLING

Quantification of the entrainment and downwind dispersion of dust and identifying the relative contributions of different sources at a receptor site is a challenge, particularly in remote regions or over large spatial areas. To better understand wind erosion patterns over large areas, wind erosion models have been developed. In previous years the wind erosion dust emission model (WE_DUST_EM) was used to evaluate dust emissions for the Williston Reservoir beaches in 2010 and 2011 dust seasons. This mesoscale model was developed to distribute wind erosion and dust emission data measured during field season research over the entire study domain. Dust emission potential (μg m^{-2} s^{-1}) measurements at the Williston Reservoir were completed using the PI-SWERL (Etyemezian et al., 2007). The dust emission relationships measured by the PI-SWERL served as input to WE_DUST_EM, and the output were mapped to show the spatial pattern of dust emission 'hot spots' to identify areas with high dust emission potential on Williston Reservoir Beaches (refer to Nickling et al., 2011, Appendix A). This successful approach remains available for use.

For 2012 a different modeling effort was undertaken to demonstrate the applicability and feasibility of a Lagrangian Particle Dispersion model (LPDM) to evaluate the relative contributions from different Williston beaches at a specific receptor site, which for our purpose is defined as a 2 km^2 area centered on the village of Tsay Keh. The receptor site can be set to any area within the Williston environment, but we chose to demonstrate the model's capability at the location where the highest number of people at any given time would potentially be exposed to levels of PM_{10} that exceeded health standards. The LDPM approach offers another method for evaluating which beaches contribute to a greater or lesser degree to a specific receptor site, such as Tsay Keh village. Using the LPDM with wind fields that are representative of those that occur in the Williston basin (event, or seasonal averages) provides an indication of which beaches contribute emitted PM to a receptor and the relative magnitude of that

contribution compared to contributions from other beaches. This information could also be used to inform a management decision whereby the beaches are ranked for priority of dust abatement measures, based on their modelled impact at a receptor.

3.1 The Lagrangian Particle Dispersal Model (LPDM)

A brief description of the LPDM is provided for informational purposes. Lagrangian models can accurately represent transport and dispersion on multiple scales and exhibit minimal numerical diffusion, but they generally do not represent complex chemical and physical transformation processes involving mixtures from multiple sources. Eulerian and Lagrangian models can be applied in source and receptor configurations. They are commonly used to track plume movements in the source-oriented mode, but they also are used to determine where pollutants come from in a receptor-oriented mode.

The main concepts of a Lagrangian particle model are described in Pielke (1984) and Rodean (1996). The basic algorithm of the model used here is as follows. Particles are released at time t at a prescribed rate and the new position at time $t + \Delta t$ of each particle is determined by using the standard random displacement method as:

$$x(t+\Delta t) = x(t)+ [u(t) +u_r(t)] \Delta t \quad (3.1)$$

$$y(t+\Delta t) = y(t)+ [v(t) +v_r(t)] \Delta t \quad (3.2)$$

$$z(t+\Delta t) = z(t)+ [w(t) +w_r(t)] \Delta t \quad (3.3)$$

where x, y, and z are the particle positions; u, v, w are predicted mean components of the velocity along the x-, y-, and z-axes, respectively; u_r, v_r and w_r are the corresponding subgrid-scale velocity components.

The subgrid-scale velocity components are iteratively determined as:

$$u_r(t)= u_r(t-\Delta t)R_u(\Delta t) + u_s(t-\Delta t) \quad (3.4)$$

$$v_r(t)= v_r(t-\Delta t)R_v(\Delta t) + v_s(t-\Delta t) \quad (3.5)$$

$$w_r(t)= w_r(t-\Delta t)R_w(\Delta t) + w_s(t-\Delta t) \quad (3.6)$$

where R_u, R_v, and R_w are the Lagrangian autocorrelation functions for each velocity component, and u_s, v_s, and w_s are the random fluctuations of the velocity components.

The Lagrangian correlation functions are calculated from:

$$R_u(\Delta t) = e^{-\Delta t/T_{Lu}} \quad (3.7)$$

$$R_v(\Delta t) = e^{-\Delta t/T_{Lv}} \tag{3.8}$$

$$R_w(\Delta t) = e^{-\Delta t/T_{Lw}} \tag{3.9}$$

where T_{Lu}, T_{Lv}, and T_{Lw} are the Lagrangian time scales for the corresponding velocity components. The time scales are determined from the following scaling arguments:

$$T_{Lu} = z_i \Big/ \sqrt{\overline{(u'u')_m}} \tag{3.10}$$

$$T_{Lv} = z_i \Big/ \sqrt{\overline{(v'v')_m}} \tag{3.11}$$

$$T_{Lw} = z_i \Big/ \sqrt{\overline{(w'w')_m}} \tag{3.12}$$

where z_i is the depth of the mixed layer, and $\overline{u'u'}_m$, $\overline{v'v'}_m$, and $\overline{w'w'}_m$ are the maximum variances in the domain. The top of *zi* is determined from the elevated minimum of the turbulence kinetic energy (TKE). The bounds for the random components are determined from the statistical properties of turbulent transfer and the following autocorrelation functions:

$$\sigma_u = \sqrt{\overline{u'u'} \cdot \{1 - R_u^2(\Delta t)\}} \tag{3.13}$$

$$\sigma_u = \sqrt{\overline{v'v'} \cdot \{1 - R_v^2(\Delta t)\}} \tag{3.14}$$

$$\sigma_w = \sqrt{\overline{w'w'} \cdot \{1 - R_w^2(\Delta t)\}} \tag{3.15}$$

where σ_u, σ_v, and σ_w are the standard deviations around zero mean for the range of random components u_s, v_s, and w_s, respectively, and and $\overline{u'u'}$, $\overline{v'v'}$, and $\overline{w'w'}$ are the variances of the velocity components in the *x*, *y*, and *z* directions, respectively. Model parameterization includes options for spatially and temporarily variable (Hanna 1982) or constant time scales (Gifford 1995), a drift correction term (Legg and Raupach, 1982), a plume rise algorithm, and three optional turbulence parameterizations (Donaldson, 1973; Mellor and Yamada, 1974; Andrén, 1990). Meteorological input to the LPDM includes 3D fields of *u*, *v*, and *w* wind components and potential temperature simulated by a 3D regional/mesoscale model. The model can be applied to multiple point, line, area, and volume sources, with the rate of particle

release for each source possibly varying in time. The specifics of the parameterizations of the LPDM used in this study are presented later.

3.2 Model Input Data

Currently the data sets representing hourly wind fields (i.e., wind speed and direction at multiple sites and heights) and PM_{10} concentrations for the Williston Reservoir during known dust events are extremely limited. A database of emission flux ($\mu g\ m^{-2}\ s^{-1}$) potential is available from the PI-SWERL testing as are data for dust emission threshold wind speeds. Combining these emission flux data with wind speed and direction data obtained during dust events at Davis beach during the tillage trials in 2009 and 2010, input data for the LDPM was developed (Table 3.1). In addition, some measure of PM_{10} at the receptor site is useful to provide corroboration of the model-calculated values. As there was no TEOM operating at Tsay Keh during the tillage trials, the 24-hour mean PM_{10} obtained with the Partisol operating at Tsay Keh beach was used to constrain and evaluate the model-predicted values.

3.2.1 Beach Delineations

To begin the modeling exercise required that the grid coordinates of all the identified beaches be established. The LDPM model requires that the shape of an area emission source must be defined as either a circle or a rectangle. For our purposes the choice of rectangular emission source areas was chosen because of its geometric simplicity. These delineations for the beach units were first approximated based on the maps of beaches and their respective soil textures as presented in Nickling et al. (2011) (their Fig. 3.1). Nineteen individual beach units were defined. To better represent the areal extent of the beach units within the modeling domain they were sub-dived into multiple rectangles to provide a more accurate representation of total area for each defined unit. Primarily the sizes and numbers of the sub-areas within a designated beach unit were defined based on the size and shape of the beach. This arbitrary procedure created 104 sub-units ranging in size from 0.055 km^2 to 21.915 km^2 (Table 3.1, Fig. 3.1). Based on the latitude and longitude of each northeast and southwest corner of a sub-unit, a rectilinear grid coordinate was assigned to each corner based on the Lambert Conformal projection. This conversion was done within Arc GIS.

3.2.2 Threshold Shear Velocity Attribution by Beach Unit

A threshold friction velocity (u_{*t}) for each beach sub-unit was based on either a mean u_{*t} for dust as measured with the PI-SWERL for the beach unit, or assigning a u_{*t} based on relating the beach soil texture to a mean PI-SWERL-derived u_{*t} from measurements on the same soil texture, but at a different location. As the LPDM does not use shear velocity it was necessary to

Table 3.1. Beach unit and sub-unit designations, areas, assigned z_0, u_{*t}, and $u_{10\ m}$ threshold wind speeds.

ID Number	Beach Unit Name	Soil Texture Classification	Beach Area (km^2)	z_0 (m)	Average u_{*t} (m s^{-1})	u_{10} Threshold (m s^{-1})
1	Raspberry S1	Sand	0.848	0.0001	0.310	8.92
2	Raspberry S2	Sand	1.058	0.0001	0.310	8.92
3	Raspberry S3	Sand	0.425	0.0001	0.310	8.92
4	Raspberry N	Sand	2.267	0.0001	0.310	8.92
5	Bob Fry 3	Silty Loam	1.191	0.0010	0.430	9.90
6	Bob Fry 2	Silty Loam	5.194	0.0010	0.430	9.90
7	Bob Fry 1	Silty Loam	2.256	0.0010	0.430	9.90
8	Bob Fry S	Clay	4.563	0.0010	0.470	10.82
9	Bob Fry N	Clay	3.543	0.0010	0.470	10.82
10	Pete Toy 1	Sand	5.550	0.0001	0.280	8.06
11	Pete Toy 2	Sand	3.470	0.0001	0.230	6.62
12	Pete Toy 3	Sand	1.749	0.0001	0.230	6.62
13	Pete Toy 4	Sand	1.639	0.0001	0.230	6.62
14	Pete Toy 5	Sand	1.165	0.0001	0.230	6.62
15	Pete Toy 6	Sand	2.557	0.0001	0.230	6.62
16	Pete Toy 7	Sand	1.906	0.0001	0.230	6.62
17	Corless B1	Sand	1.003	0.0001	0.250	7.20
18	Corless B2	Sand	0.921	0.0001	0.250	7.20
19	Corless B3	Sand	2.075	0.0001	0.250	7.20
20	Corless B4	Sand	0.259	0.0001	0.250	7.20
21	Corless B5	Sand	0.545	0.0001	0.250	7.20
22	Corless A1	Sand	0.088	0.0001	0.260	7.48
23	Corless A2	Sand	0.300	0.0001	0.260	7.48
24	Corless A3	Sand	0.915	0.0001	0.260	7.48
25	Corless A4	Sand	0.432	0.0001	0.260	7.48
26	Corless A5	Sand	0.234	0.0001	0.260	7.48
27	Corless A6	Sand	0.216	0.0001	0.260	7.48
28	Corless A7	Sand	0.296	0.0001	0.260	7.48
29	Corless A8	Sand	0.591	0.0001	0.260	7.48
30	Corless A9	Sand	0.523	0.0001	0.260	7.48
31	Corless A10	Sand	0.642	0.0001	0.260	7.48
32	Corless A11	Sand	0.179	0.0001	0.260	7.48
33	Corless A12	Sand	0.252	0.0001	0.260	7.48
34	Corless A13	Sand	0.823	0.0001	0.260	7.48
35	Corless A14	Sand	0.263	0.0001	0.260	7.48
36	Northwest 1	Sand	0.053	0.0001	0.290	8.35

37	Northwest 2	Sand	0.481	0.0001	0.290	8.35
38	Northwest 3	Sand	0.297	0.0001	0.290	8.35
39	Northwest 4	Sand	0.238	0.0001	0.290	8.35
40	Northwest 5	Sand	0.222	0.0001	0.290	8.35
41	Northwest 6	Sand	0.232	0.0001	0.290	8.35
42	Northwest 7	Sand	0.250	0.0001	0.290	8.35
43	Northwest 8	Sand	0.331	0.0001	0.290	8.35
44	Northwest 9	Sand	0.224	0.0001	0.290	8.35
45	Ingenica S	Sand	0.162	0.0001	0.290	8.35
46	Ingenica N1	Sand	0.134	0.0001	0.290	8.35
47	Ingenica N2	Sand	0.242	0.0001	0.290	8.35
48	Northwest 10	Sand	0.347	0.0001	0.290	8.35
49	Northwest 11	Sand	0.420	0.0001	0.290	8.35
50	Tsay Key 1	Loamy Sand	0.131	0.0010	0.400	9.21
51	Tsay Key 2	Loamy Sand	0.085	0.0010	0.400	9.21
52	Tsay Keh 3	Loamy Sand	1.802	0.0010	0.400	9.21
53	Tsay Keh 4	Sandy Loam	0.381	0.0001	0.270	7.77
54	Tsay Keh 5	Sandy Loam	1.681	0.0001	0.270	7.77
55	Tsay Keh 6	Sandy Loam	0.079	0.0001	0.270	7.77
56	Tsya Keh 7	Loamy Sand	0.086	0.0010	0.400	9.21
57	Tsay Keh 8	Sand	0.156	0.0001	0.290	8.35
58	Van Somer	Sand	1.698	0.0001	0.290	8.35
59	Northeast 1	Sand	0.064	0.0001	0.290	8.35
60	Northeast 2	Sand	0.099	0.0001	0.290	8.35
61	Northeast 3	Sand	0.209	0.0001	0.290	8.35
62	Northeast 4	Sand	0.396	0.0001	0.290	8.35
63	Northeast 5	Sand	0.170	0.0001	0.290	8.35
64	Northeast 6	Sand	0.100	0.0001	0.290	8.35
65	Northeast 7	Sand	0.147	0.0001	0.290	8.35
66	Northeast 8	Sand	0.148	0.0001	0.290	8.35
67	Northeast 9	Sand	0.434	0.0001	0.290	8.35
68	Northeast 10	Sand	0.603	0.0001	0.290	8.35
69	Northeast 11	Sand	0.106	0.0001	0.290	8.35
70	Northeast 12	Sand	0.087	0.0001	0.290	8.35
71	Northeast 13	Sand	0.158	0.0001	0.290	8.35
72	Northeast 14	Sand	0.107	0.0001	0.290	8.35
73	Northeast 15	Sand	0.253	0.0001	0.290	8.35
74	Northeast 16	Sand	0.231	0.0001	0.290	8.35
75	Northeast 17	Sand	0.205	0.0001	0.290	8.35
76	Northeast 18	Sand	0.062	0.0001	0.290	8.35
77	Northeast 19	Sand	0.125	0.0001	0.290	8.35

78	Northeast 20	Sand	0.163	0.0001	0.290	8.35
79	Middle Creek N1	Sand	0.849	0.0001	0.320	9.21
80	Middle Creek N2	Sand	9.052	0.0001	0.320	9.21
81	Middle Creek S	Sand	3.088	0.0001	0.310	8.92
82	Shovel	Sand	4.443	0.0001	0.220	6.33
83	Davis N1	Sandy Loam	5.269	0.0001	0.240	6.91
84	Davis N2	Sand	5.467	0.0001	0.290	8.35
85	Davis S1	Sand	1.109	0.0001	0.275	7.92
86	Davis S2	Loamy Sand	2.219	0.0001	0.300	8.63
87	Davis S3	Sand	1.607	0.0001	0.275	7.92
88	Davis S4	Sand	0.053	0.0001	0.275	7.92
89	Davis S5	Sand	2.599	0.0001	0.275	7.92
90	Bruin Creek 1	Loamy Sand	2.318	0.0001	0.300	8.63
91	Bruin Creek 2	Loamy Sand	5.694	0.0001	0.300	8.63
92	Collins N1	Sand	5.501	0.0001	0.310	8.92
93	Collins N2	Sand	2.120	0.0001	0.310	8.92
94	Collins N3	Loamy Sand	1.380	0.0001	0.280	8.06
95	Collins N4	Loamy Sand	4.398	0.0001	0.280	8.06
96	Collins N5	Silty Loam	8.696	0.0001	0.430	12.38
97	Collins S1	Sandy Loam	17.411	0.0001	0.270	7.77
98	Collins S2	Sand	2.697	0.0001	0.310	8.92
99	Lafferty 1	Sandy Loam	7.305	0.0001	0.270	7.77
100	Lafferty 2	Sand	2.624	0.0001	0.310	8.92
101	Ospika N	Sand	6.929	0.0001	0.360	10.36
102	Ospika S2	Sand	21.915	0.0001	0.360	10.36
103	Ospika S	Sand	12.119	0.0001	0.360	10.36
104	Bevel Creek	Loamy Sand	3.008	0.0001	0.220	6.33

Figure 3.1. The locations of the designated beach units and their assigned soil texture. Note that for modelling purposes beach size is represented by a rectangle of equivalent size to the irregular shaped beach area.

convert the u_{*t} value to a wind speed at 10 m. This was accomplished by using the observed roughness lengths measured during the 2009 and 2010 tillage trials by the meteorological tower on Davis beach. Beaches with low u_{*t} values were assigned a roughness length (z_0) of 0.0001 m and beaches with higher u_{*t} values were assigned a z_0 value of 0.001 m, so that they would begin to emit at higher regional wind speeds.

3.2.3 Wind Data

Four sets of wind data were developed for this modeling exercise. The first is a synthetic data set use to represent a simple typical storm event that lasted for 12 hours with wind speeds ranging from ≈12 m s^{-1} to ≈18 m s^{-1} measured at 10 m above ground level (AGL), increasing during the first eight hours and diminishing over the last four hours (Fig. 3.2). Over the same time interval the winds changed direction 2° for the first 4 hours beginning with an azimuth of 140° veering to 148°, holding steady for two consecutive hours and then declining 2° for the next six hours, ending with the azimuth 138°. This was assumed to represent a wind event from the south that would initiate dust emissions on the beach and its subsequent transport to the north under a simple pattern of varying wind speed and direction. The model was run an additional 24 hours repeating the 12-hour wind direction pattern and with winds below threshold for emissions to allow for particles emitted from the beaches to complete the transport phase to the receptor site (Fig. 3.2).

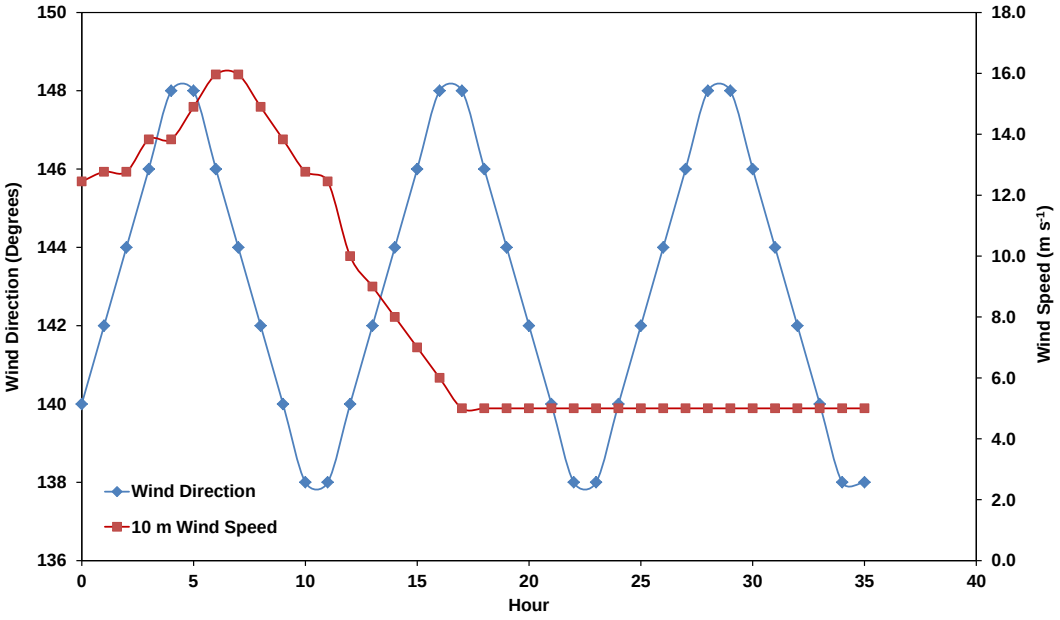

Figure 3.2. The synthetic wind field data representing a 12 hour dust emission event followed by a period of winds below threshold with an oscillating wind direction originating from the south west.

The other three data sets for wind were based on actual dust transport events measured on Davis beach: 29-5-2009 (6 hours), 5-24-2010 (12 hours), and 2-6-2010 (3 hours) (Fig. 3.3). For each wind field data set the vector wind speeds (i.e., *u*, *v*, and *w*) at 1 m, 10 m, and 50 m AGL must be estimated for input into the LPDM. The *u* and *v* components were calculated as:
$u = u_z \times \sin(WD)$ and $v = u_z \times \cos(WD)$, where u_z is measured wind speed at height z and WD is wind direction. As no measurements of *w* were taken, appropriate values based on the model predicted turbulent kinetic energy were used as input. It must be noted that in this simple modeling approach that the wind speed and direction applies equally throughout the modelling domain. In reality there would be considerable variability in these parameters created by the local topography and if accounted for the results could be quite different. At this time there is only limited data on wind speed and direction in the modeling domain and it is being accumulated as part of the on-going Air Quality Monitoring program. These data will be valuable in the future for improving the quality of the modeled dust attribution from the identified beach units.

3.2.4 Dust Flux Data

Hourly dust flux in g s^{-1} was calculated for each sub-unit of beach once threshold was reached based on PI-SWERL derived measurements. The emission flux for each sub-unit was calculated using the general equation F (µg m^{-2} s^{-1}) = au_*^b, where *a* and *b* are coefficients from PI-SWERL derived F vs. u_* relationships for each beach unit if measurements were available. In the absence of measurements, flux was estimated based on the assigned texture of the beach and PI-SWERL measured relationships on beaches of similar texture. As u_* is required to generate a dust flux it was calculated for every hour of the dust event outside the LPDM environment using the hourly measured wind speed (e.g., Figs. 3.2 and 3.3) and roughness length (z_0) values based on estimates from the vertical wind speed profile measurements made on Davis beach during the tillage trial testing of 2009-2010 and applying the "log law" (Prandtl, 1935):

$$\frac{u_z}{u_*} = \frac{1}{\kappa} ln\left(\frac{z}{z_o}\right) \tag{3.16}$$

where κ is the von Kármán constant (0.4). With an hourly u_*, F could be calculated for each of the 104 beach sub-units. For simplicity, and due to a lack of wind speed data from other parts of the Williston reservoir, we assume that the wind speed at 10 m measured at Davis beach is the same over the entire modeling domain. The emissions in g s^{-1} for each beach sub-unit are calculated by dividing F by its area.

The model was first run using the synthetic wind data and PM_{10} emission data for each beach sub-unit to evaluate the mathematical stability of the solutions of the equations and tune model parameters before using actual wind data were used to simulate an observed dust transport event. The tuning exercise is most critical for developing the appropriate particle

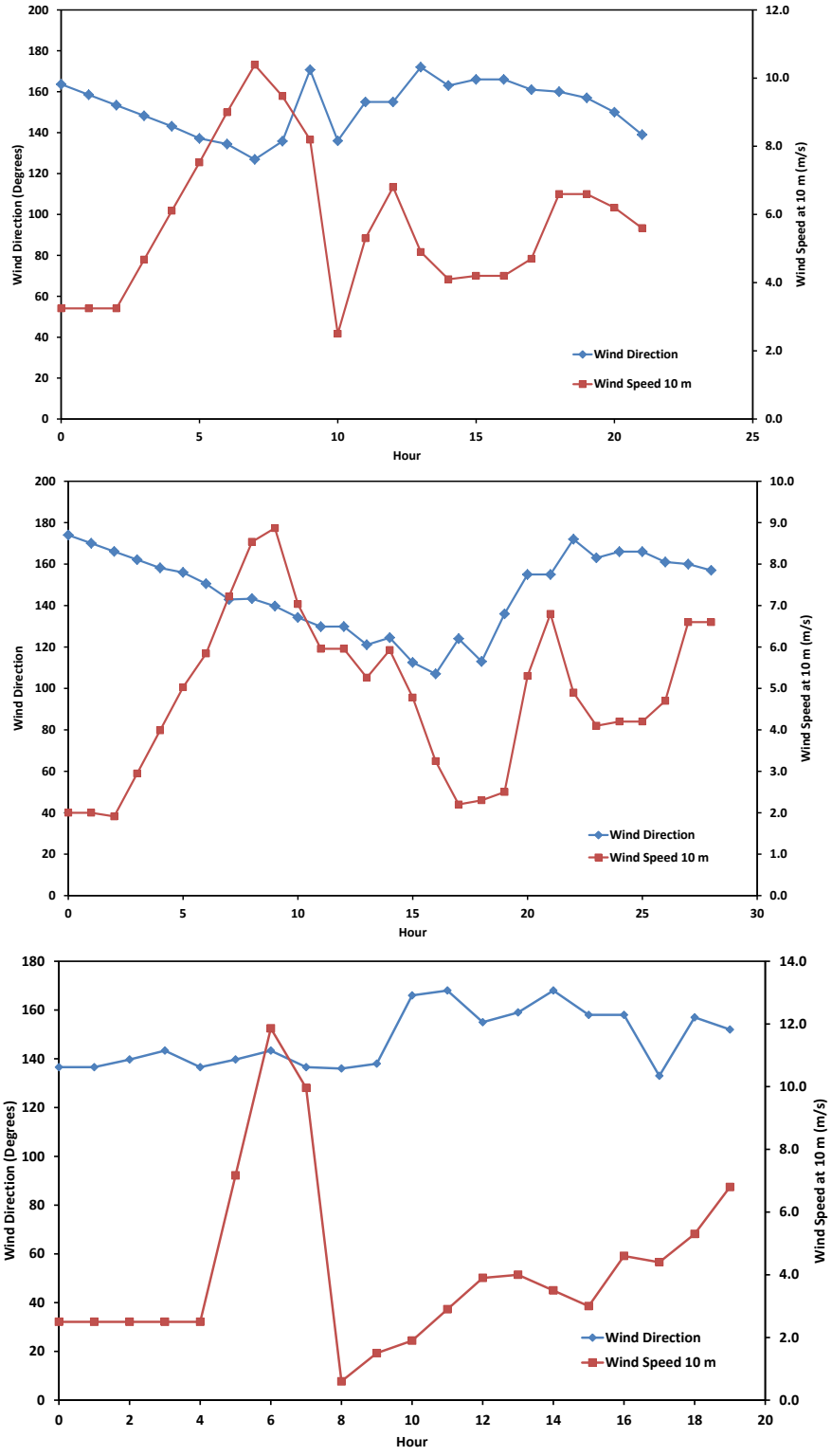

Figure 3.3. Wind directions and wind speeds during dust events measured on Davis beach 29-5-2009 (top panel) and 24-5-2010 (middle panel), and 2-6-2010 (bottom panel).

number emission rates that may have to be adjusted so that during model calculation it matches, within reason, the mass emission rate and provides mathematical stability to the solutions of the equations.

3.3 Model Results

3.3.1 Synthetic Wind Test Conditions

The model estimates of PM_{10} concentrations at the receptor site (i.e., Tsay Keh village) during the duration of the synthetic dust emission and transport event is shown in Fig. 3.3. The model output shows that the PM_{10} at Tsay Keh steadily rises from the initiation of dust emissions through to approximately the seventh hour of the even. This period of increasing PM_{10} represents that period when the emissions from the near sources first begin to contribute to the dust followed by a transport period that finally brings the dust emitted furthest from the receptor into the receptor environment. Following this the concentration pattern reflects, to a large degree, the imposed wind direction pattern (Fig. 3.1). The modelled concentrations show the synthetic winds create PM_{10} levels that are realistic in terms of measured values at the Tsay Keh beach Partisol that was operated during 2009 and 2010, giving confidence that the particle number emission rates were adequately representing the mass emission rates as measured by the PI-SWERL.

As Fig. 3.4 shows the dust arriving at Tsay Keh under these imposed wind conditions is predominantly from four source areas, which are designated in the beach units as all being part of Tsay Keh beach (Table 3.1). This is not an unexpected result as the Tsay Keh beach units represent emission sources closest to the receptor and therefore will, under these simple meteorological conditions, dominate the PM_{10} concentration received at the designated receptor site. Dispersion processes operate to reduce the contributions of dust from sites further away.

A measure of the relative contributions from each of the 104 beach sub-unit source areas can also be estimated from the model output. For the synthetic wind data the final attribution of average concentration by source is shown in Figure 3.5. For these synthetic test data the results show that only six of the 104 delineated source areas contribute appreciably (i.e., >0.5% of the total) to the model-predicted average concentration at the receptor site (i.e., Tsay Keh). The single largest contributor is the Tsay Keh beach complex (units 51-57).

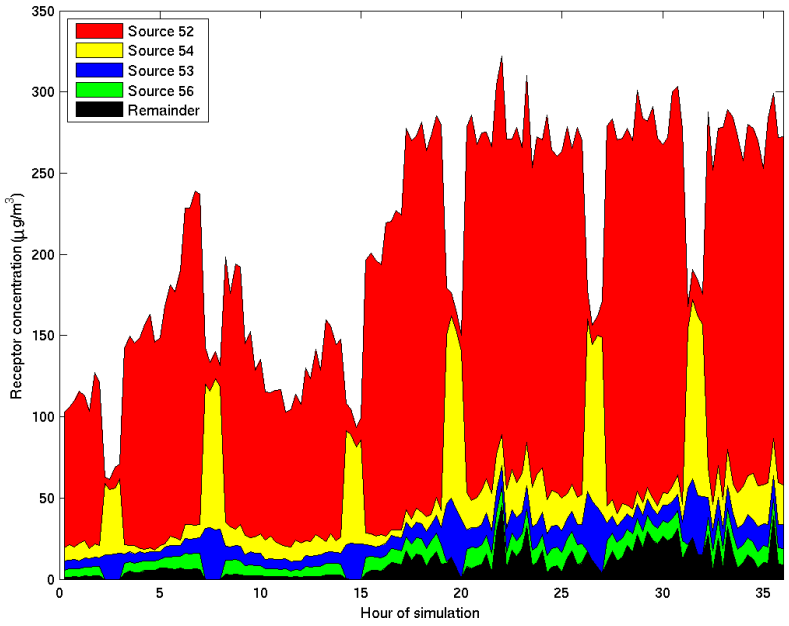

Figure 3.4. Modelled PM_{10} levels at Tsay Keh receptor for the synthetic wind data representing a simple storm event.

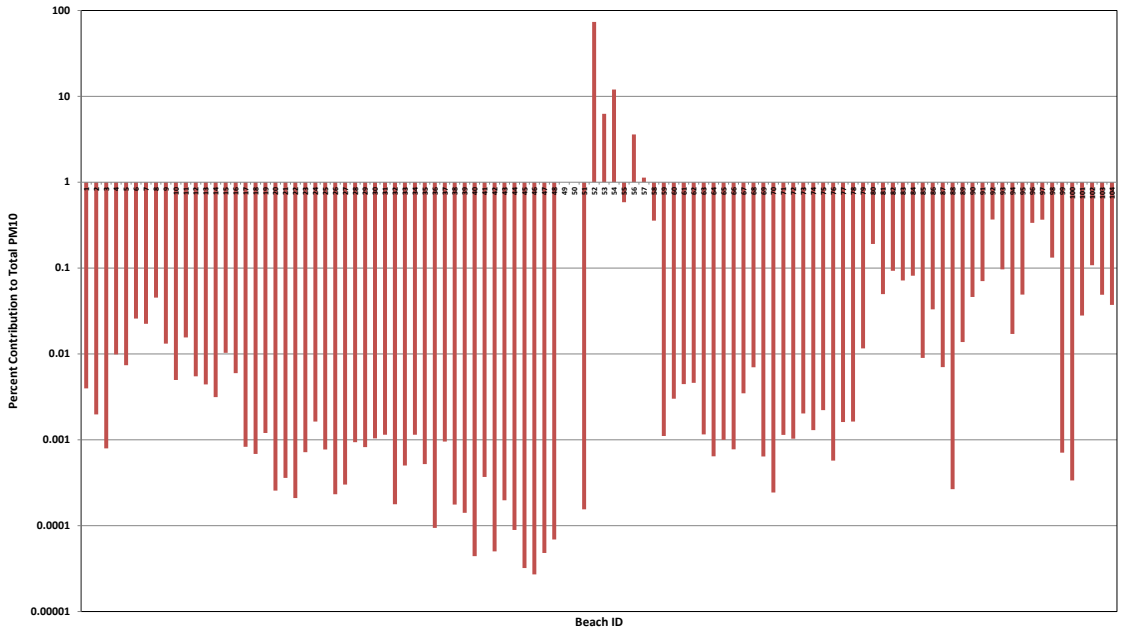

Figure 3.5. The percentage contribution to the total (modelled) PM_{10} for the identified 104 beach sub-units to the Tsay Keh receptor site. Beach number corresponds to the list in Table 3.1. The y-axis is in a logarithmic scale to allow the low contributors to be seen on the plot.

3.3.2 Davis Beach Dust Event Winds

The approach using the synthetic data is subsequently applied for the three dust emission and transport events based on measurements of wind speed and directions from the Davis beach measurements made during the 2009 and 2010 tillage trials. In the supplied Figures note that the Y-axis for the percent contribution to total PM_{10} mass modelled for the receptor site plots is plotted as a logarithm, which for values <1 means the longer the bar the lower the contribution. This plotting method was chosen so that the contributions from each beach unit could be visualized.

3.3.2.1 Dust Event of 29-5-2009

The dust emissions generated within the LPDM for 29-5-2009 are based on the wind speed and direction patterns shown in Fig. 3.3 (top panel). For this case ten beaches contribute greater than 1% each to the total amount of PM_{10} received at the receptor site of Tsay Keh (Fig. 3.6). The Tsay Keh beach units (52, 53, 54, 55, and 57) contribute 43% of the total. Van Somer beach (unit 58) contributes substantially as well accounting for 44% of the total PM_{10} at Tsay Keh. The beach units designated as Northeast (59, 60, 61, and 62) combine to contribute 11% of the total. The contribution from Van Somer beach appears in this case as the winds are more southerly than in the case of the synthetic wind field data, indicating that this beach is a good candidate for prioritizing for control by tillage. Care should be given to ascribing much validity to attributions from individual beach units <0.1%, which suggests that in this case no beach unit on the west side of the reservoir contributed a measureable amount until beach unit 50 is reached, which is part of the Tsay Keh beach complex and close to the designated receptor. On the east side, beach units designated as part of the Northeast complex approach this criterion (unit 63 reaches it) and unit 83, which is part of the Davis South complex also meets this criterion.

3.3.2.2. Dust Event of 24-5-2010

The dust event of 24-5-2010 is driven in the model by the wind speed and wind direction shown in the middle panel of Fig. 3.3. In this case the wind direction veers even further to the south than the event of 29-5-2009. The result is that more of the beach units on the eastern side of the reservoir make measureable contributions of >0.1% to the Tsay Keh receptor site, although the Tsay Keh beach units still dominate as the contributing source areas (Fig. 3.7). The Tsay Keh units (52-57) contribute 88% to the total PM_{10}. Van Somer (unit 58) contributes 4%. Further south the Northeastern designated beach units (59-78) contribute to 4% of the total PM_{10} and the Middle Creek complex (79-81) and Davis Beach units contribute 1.2% and 0.6%, respectively.

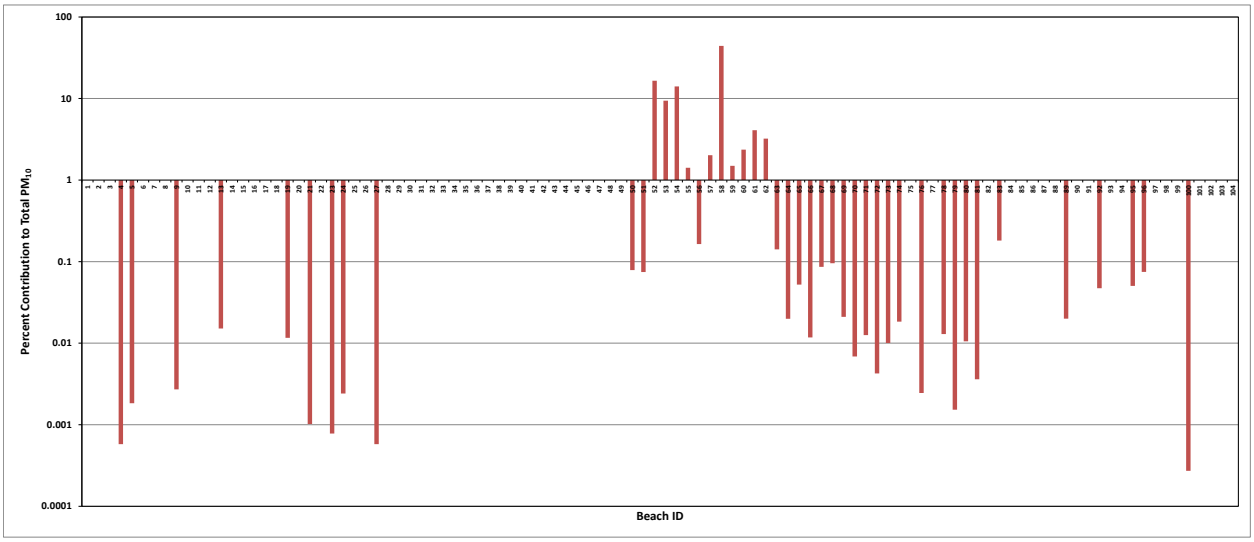

Figure 3.6. The percentage contribution to the total (modelled) PM_{10} for the identified 104 beach sub-units to the Tsay Keh receptor site for the 29-5-2009 emission event. Beach number corresponds to the list in Table 3.1. The y-axis is in a logarithmic scale to allow the low contributors to be seen on the plot.

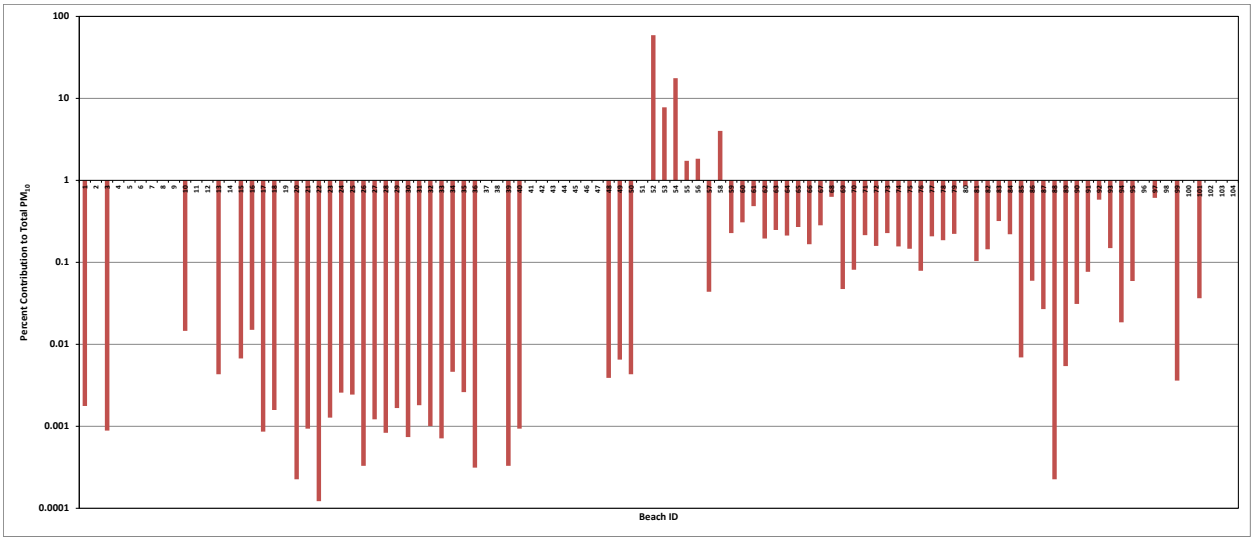

Figure 3.7. The percentage contribution to the total (modelled) PM_{10} for the identified 104 beach sub-units to the Tsay Keh receptor site for the 24-5-2010 emission event. Beach number corresponds to the list in Table 3.1. The y-axis is in a logarithmic scale to allow the low contributors to be seen on the plot.

3.3.2.2. Dust Event of 2-6-2010

The dust event of 2-6-2010 is driven in the model by the wind speed and wind direction shown in the bottom panel of Fig. 3.3. As in the other test cases the beach units in the Tsay Keh complex contribute the largest proportion of PM_{10} to the total observed mass concentration at the Tsay Keh receptor site (Fig. 3.8). In addition for this event contributions of significance were observed to originate from the Collins Beach complex (units 92, 93, 95, 97, and 98). Beach units as far south as Ospika (101, 102, and 103) on the eastern side of the reservoir contribute to 0.9% of the total. It should be recognized that in the absence of the Tsay Keh beaches sources the contributions from all other sources would not be sufficient to cause an exceedance of air quality guideline values at the Tsay Keh receptor site. This illustrates that dispersion of the particulate matter emissions over long distances is a powerful mitigating factor for reducing ambient concentration of PM_{10} at the receptor site.

In this case contributions that exceed 0.1% of the total PM_{10} are observed to occur from beaches on the western side of the reservoir including Bob Fry (units 6 and 8), and Pete Toy (units 10 and 11). These represent, in the case of Bob Fry a clay texture soil, and in the case of Pete Toy the largest units of sandy soils on the western side. Care should be taken not to over-ascribe importance to Bob Fry at this point as the emission flux is based on a small sampling of that beach unit with the PI-SWERL (Fig. 2.17). In addition the estimated contributions are at levels that would not compromise air quality at the receptor site.

As for the other test cases it appears that for the most part, at least under the very limited wind fields used in this initial modeling effort that the contributions from beach units on the western side of the reservoir are of reduced importance to those on the eastern side. This principally reflects their smaller areal extents. It must be noted however, the wind field pattern on the western side of the reservoir may not be as closely aligned with that on the eastern side, which was imposed in this modelling exercise.

3.4 Modelling Challenges and Recommendations

The greatest challenge to improving the modelling of dust emission and transport within the Williston Reservoir environment is improving the quality of the wind data input and increasing the data record length (and potentially the spatial distribution) of PM_{10} measurements. Wind data of known quality are required to drive the meteorological components of dispersion models and to provide a means to estimate the surface shear stress, which controls the threshold of emissions as well as their strength. Measurements of PM_{10} are needed to reconcile the model predictions with observed values to provide a means to check the plausibility of the modelled values.

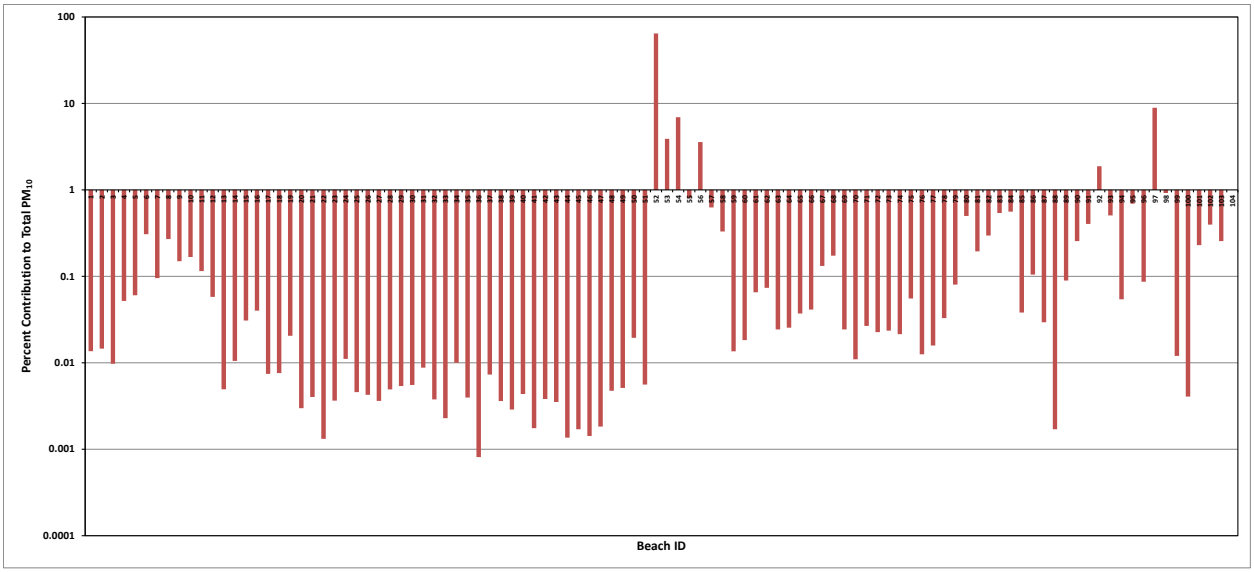

Figure 3.8. The percentage contribution to the total (modelled) PM_{10} for the identified 104 beach sub-units to the Tsay Keh receptor site for the 2-6-2010 emission event. Beach number corresponds to the list in Table 3.1. The y-axis is in a logarithmic scale to allow the low contributors to be seen on the plot.

Wind data that characterizes its speed at multiple vertical heights and its direction across the topography of the reservoir and its surrounding environment (i.e., up to and including the north south mountain ranges) are necessary to provide realistic conditions to evaluate surface shearing stress on the beaches. A measure of shear stress is required to evaluate if threshold for sand transport and dust emissions is reached and to apply the measured PM_{10} emission relationships (from PI-SWERL) to estimate the strength of the emissions ($\mu g\ m^{-2}\ s^{-1}$) from each defined beach unit. These are converted to $g\ s^{-1}$ for each beach unit for input into the LPDM. Higher resolution wind speed and direction data are required for the model to more realistically transport the emitted PM_{10} to a receptor site. In the modeling effort reported here wind speed and wind direction were uniform across the reservoir for each hour of simulation. This is of course a very simplified version as we know that wind speed and direction will not be uniform across such a large modeling domain, but will be affected by regional and even very local topography.

The record of PM_{10} concentration data at multiple receptors over multiple years during dust events is, at present, extremely limited. There is one year of near continuous hourly PM_{10} (and meteorology data) for Tsay Keh and Fort Ware (2012) (with another year's data becoming available for 2013), but these are of limited use to use to develop a deeper understanding of the dust storm climatology of the Williston reservoir as they are not long enough records to characterize the system behavior. In addition, the PM_{10} monitoring on the east and west shorelines is not at the required temporal frequency to allow for characterizing hourly PM_{10}

concentrations across space. This network would better serve modeling of the dust emissions if it could be upgraded to operate on a daily basis with one hour average PM_{10} resolution. This would also allow for better characterization of predicted PM_{10} levels, using modeling, for receptor sites other than Tsay Key (or Ft. Ware), which is an identified area of concern voiced by Tsay Keh leaders. There is instrumentation available that could be integrated into the regional air quality monitoring network to provide hourly PM_{10} concentration data, but this would require additional resources of capital and labour be applied to executing this modification.

Several options can be considered to improve the current limits to developing a robust dust modeling system for the Williston Reservoir. To increase the quality of the meteorological input data several options are available: 1) increase the measurement of key meteorological parameters with additional instrumentation, 2) investigate using modelled wind field data, or 3) use modelled data with on-the-ground verification measurements. It would also be appropriate to have periodic measurements of the emission potential of select beaches, using PI-SWERL for example, to determine if the range observed to date is characteristic of the system or that its range extends above what has been measured.

There are several helpful ways that the LDPM could be used in the future to aid in the dust mitigation strategy for the Reservoir. For example, the model could be run for identified dust events, which would allow for a characterization of which beaches most frequently affect air quality at a receptor and their relative contributions to the PM_{10} within a receptor zone. This could be initiated by first identifying dust events in the air quality monitoring record and then acquiring the associated meteorological data that characterized the dust event. One source of data that may be worth examining is that available through the SpotWx portal (spotwx.com) that serves as an access point to various model-derived data for the Williston Reservoir. From identified meteorological events that produced dust emissions the LPDM could be used to generate the relative contributions of PM_{10} from each beach unit to an identified receptor site, such as Tsay Kay village. By accumulating LDPM model output for identified dust storms the data will reveal how the meteorology affects emission, transport, and dispersion of the emitted dust from each beach unit, and be useful to develop a rank order for which beaches affect the receptor based on the frequency of impact and/or the magnitude of their contributions.

To illustrate this concept Fig. 3.9 shows the average rank order of contribution of PM_{10} from beaches to the Tsay Keh receptor site using the four dust emission test cases described earlier. Figure 3.9 shows that, on average, the greatest single contributor to PM_{10} at Tsay Keh is beach unit 52, followed by the rest of the Tsay Keh beach complex units. The highest ranked contributor outside of the Tsay Keh complex is unit 92 (ranked 7^{th}), part of the Collins beach

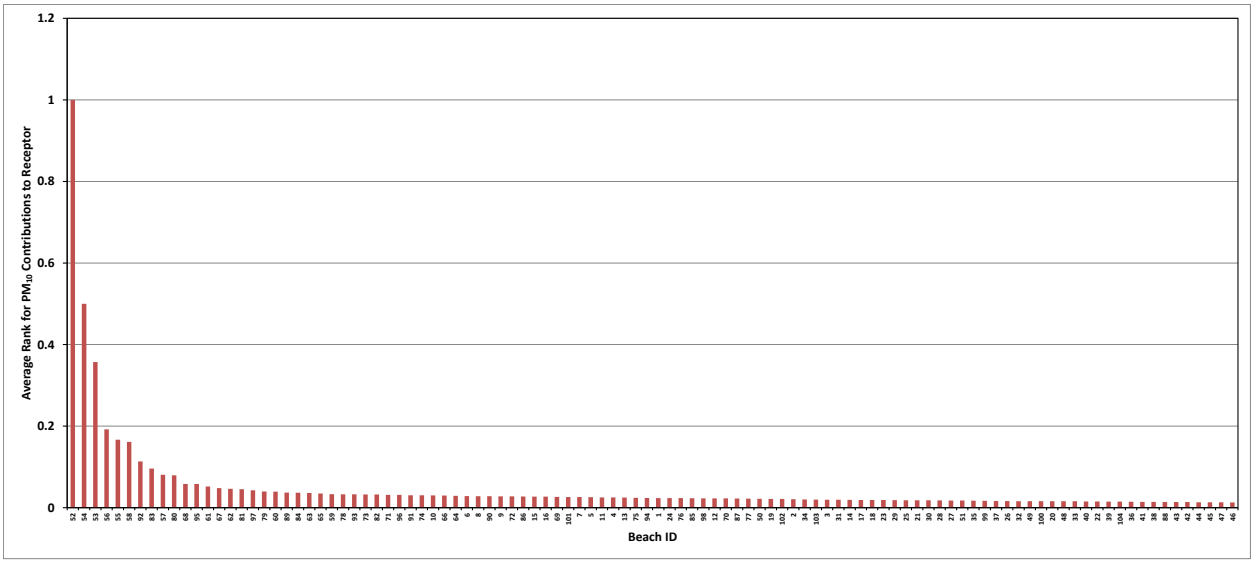

Figure 3.9. The average rank order of contribution of PM_{10} from beaches to the Tsay Keh receptor site using the four dust emission test cases

complex followed by unit 83 (8^{th}), which is part of the Davis Beach complex. The power of this approach to define the rank contribution to a specific receptor grows with the length of the data record that characterizes the dust climatology of the reservoir, which is defined by the regional wind speed and direction patterns and the emission strength of the beach units. The limited amount of model data shown in Fig. 3.9 should not be used to define the present conditions at Williston, it is presented here for illustrative purposes only.

Other models for generating wind fields in the reservoir, in particular CALMET has previously been used to good success to use in the wind erosion dust emission model (WE_DUST_EM) described in Nickling et al. (2010, 2011). CALMET is the meteorological component of the CALPUFF air dispersion modelling system (url: http://www.src.com/calpuff/calpuff1.htm, accessed Jan. 17/12). CALMET offers several pre-processing algorithms to convert common data formats for meteorological, land use and elevation data sets used in the United States into input files for the CALMET model. However, as noted in Nickling et al. (2011) it is not straightforward to use in the context of Williston Reservoir as there are no pre-processors that read the data formats available in Canada, and some of these pre-processors do not accept user-defined data sets. Therefore, for applications outside of the United States most of input data must be manually reformatted and sometimes manually constructed before it can be used in CALMET. The manual generation of these files is a time consuming task. Once all the input files for CALMET have been generated the model is used to generate hourly wind field grids with algorithms that utilize surface and upper air meteorological data including wind speed and direction, air temperature and pressure, relative humidity, cloud ceiling and cover along with surface elevation and land cover data.

Information on the frequency and magnitude that individual beaches (or beach complexes) impact a receptor site could be used to aid in dust management decisions. For example, if Tsay Keh (village) was designated a priority for minimizing exposure of people to PM_{10} dust, it may be of reduced value to focus resources on controlling beaches at a critical distance to the south as the model may show that they minimally contribute to the PM_{10} burden at Tsay Keh. The model could show which beaches, given the known range of meteorological conditions that occur during dust emissions events, affect air quality to the greatest extent for a given set of criteria (e.g., greatest population exposure, highest density of family campsites, etc.). This information could be used to develop management decisions for targeting of resources to reduce the PM_{10} burden in different parts of the reservoir environment, while reducing mitigation efforts for beaches that have minimal effect on areas that are not deemed sensitive to human activities (i.e., areas with low probability of exposure due to low use).

The rank ordering of beaches to characterize the frequency and or magnitude they impact a receptor will likely change over time. By using each year's dust events this can be continually adjusted, but it seems highly probable that regardless of the year-to-year variations in dust event meteorology a hierarchy of beaches will reveal a pattern that identifies the beaches that are consistent or persistent contributors to receptors that have PM_{10} levels that are above federal or provincial air quality guideline values.

4 CONCLUSIONS

This project began with the objective of assessing the feasibility of developing a model system that would identify the emission potential of beaches around the Williston Reservoir, which could lead to a system capable of providing information on the emission potential of the beaches through time and as a function of environmental conditions. This objective was fulfilled with the development of the WE_DUST_EM model. WE_DUST_EM uses relatively few input parameters and the methodology developed to obtain these input parameters using *in situ* measurements of emission potential (from PI-SWERL), GIS, and remote sensing techniques along with a stochastic approach for assessing threshold shear velocity can be applied not only to this location, but to other locations as well. The model is not without limitations, the most obvious ones being: 1) it requires considerable operator knowledge to run, 2) obtaining the data for the surface texture parameter input using LandSat databases is based on a simple algorithm developed by Xiao et al. (2006) that uses the red, blue, and green reflectance bands, and 3) it is challenging to use the CALMET model to generate the wind fields due mainly to the incompatibility of available Canadian wind data file formats with the CALMET architecture.

The model was used to estimate dust emission strength for known dust events at the Williston Reservoir for 2009, 2010, and 2011 based on the relationships for threshold shear velocity and

PM_{10} emission potential developed using the PI-SWERL for specific beaches and by extending those relationships based on soil texture (from LandSat data) to other beaches of the reservoir. The results of this multi-year modeling effort revealed that the modelled emission rates across the reservoir changed from year to year mainly due to differences in meteorology. The modelled emission rates were lower for the 2011 season than they were for the 2010 season, agreeing with the results from the 2011 air quality monitoring study. This was attributed to the lack of sustained high wind speeds associated with storms, which were more prevalent in 2010, but not observed in the 2011 field season. The modelling also revealed that there appears to be a consistent pattern of high emission beaches identified as: Collins, Davis, Shovel, and Middle Creek.

In addition to the development of the WE_DUST_EM model several important conclusions can be made based on the results of in situ measurements made as part of this project. Testing with PI-SWERL revealed how components of the dust emission system changed through time and over space for the Williston Reservoir beaches, which was unknown prior to this study. Year-to-year variation in threshold shear velocity (u_{*t} for sand and dust) was observed to occur at the same locations through time. The four years of emission potential measurements obtained with the PI-SWERL indicate that, even taking the observed variability into account, there are beaches that have a consistently higher emission potential than others. Consistently high emission beaches are: Shovel, Tsay Key, Davis N, Middle Creek N, Middle Creek S, and Collins. Other high emitting beaches based on one year of measurement were: Ruby Red, Lafferty, Bevel, Davis S, Stromquist and Chowika. These data suggest that due consideration be given to prioritizing mitigation treatments to those beaches listed in the first grouping. In addition, due to the proximity of Tsay Keh village to the potentially high emitting Tsay Keh beach it is suggested that this beach always be afforded a high priority for application of dust mitigation methods.

Another result that came to light as part of this project was the variability of dust emission potential of the beaches. Some of the beaches, notably Davis N, Collins, Tsay Key, Corless B, and Lafferty, have exhibited a high degree of variability in emission potential while others have not (e.g., Coreless A, Ospika, Pete Toy, and Shovel) at this time however, the cause of the variability in dust emission potential remains unknown. It is suggested that the cause is related to the phase of deposition of fine sediments through the water column following high pool and thereafter during the draw down phase. This is likely a complex interaction between the amount of fine particles delivered to the reservoir by the rivers and streams, as well as bank erosion inputs, and the delivery of those suspended particles to the different beaches by wind driven currents in the reservoir and their interaction with the bathymetry of the reservoir and the near shore environment. The spatial distribution of the depositional flux of suspended

sediments in the water column to the beaches could be evaluated with a measurement program.

As part of the last year of this feasibility study a different modelling approach was used, the Lagrangian Particle Dispersion Model, to evaluate its usefulness to provide information on the frequency and magnitude of different beaches to impact a specific receptor site, in this case the population center of Tsay Keh. Using available meteorological data from dust storm events measured on Davis beach during the tillage trials (Nickling et al., 2009, 2010) the LDPM model was used to characterize the potential contributions to PM_{10} at the receptor site of Tsay Keh village. The limited data indicates that near-village beaches are the most significant contributors to PM_{10} levels caused by dust emissions. The limited data also shows that beaches on the east side contributed more PM_{10} than those on the west.

The LPDM model shows promise as means to identify the relative impacts of the different beaches on a selected receptor site. It must also be noted that the current version of the LDPM used in this study is not commercially available, and requires a high-degree of operational skill and user experience to generate model output of high quality. It must be cautioned that the results presented are by no means a comprehensive evaluation of the actual impact of individual beaches due to the very simplistic treatment of wind speed and direction across the modeling domain. In order to improve the analytical capability of the LPDM it would be critical to improve the characterization of the wind fields and stability conditions that occur during actual dust transport events. The strongest evidence of which beaches potentially contribute the greatest quantities of dust and should be given a high degree of consideration for control are those identified as consistent high emitters by PI-SWERL measurements.

CITED REFERENCES

Andrén, A. 1990. Evaluation of a turbulence closure scheme suitable for air-pollution applications. J. Appl. Meterol., 29: 224-239.

Bacon, S.N., McDonald, E.V., Amit, R., Enzel, Y., and Crouvi, O. 2011. Total suspended particulate matter emissions at high friction velocities from desert landforms. J. Geophys. Res., 116 (F3): F03019.

Donaldson, C.P. 1973. Three-dimensional modeling of the planetary boundary layer. In Proceedings of a Workshop on Micrometeorology; Haugen, A., Ed.; American Meteorological Society: Boston, MA.

Etyemezian, V., Nikolich, G., Ahonen, S., Pitchford, M., Sweeney, M., Purcell, R., Gillies, J. and Kuhns, H. 2007. The Portable In-Situ Wind ERosion Laboratory (PI-SWERL): A new method to measure PM_{10} windblown dust properties and potential for emissions. Atmospheric Environment, 41: 3789 – 3796.

Gifford, F.A. 1995. Some recent long-range diffusion experiments. J. Appl. Meterol., 34: 1727-1730.

Gillies, J.A. 2013. Fundamentals of aeolian sediment transport | dust emissions and transport – near surface. In Treatise on Geomorphology, Shroder, J. (ed. in chief) and Lancaster, N. (ed.), Vol. 11: 43-63, Academic Press, San Diego, CA,

Hanna, S.R. 1992. In Atmospheric Turbulence and Air Pollution Modeling; Nieuwstadt, F.T.M., Van Dop, H., Eds.; Kluwer: Dordrecht, The Netherlands.

Kavouras, I.G., Etyemezian, V., Nikolich, G., Young, M., Gillies, J. and Shafer, D. 2009. A new technique for characterizing the efficacy of fugitive dust suppressants. Journal of the Air & Waste Management Association, 59: 603-612.

Koracin, D., Vellore, R., Lowenthal, D.H., Watson, J.G., Koracin, J., McCord, T., DuBois, D.W. and Chen, L.-W.A. 2011. Regional source identification using Lagrangian stochastic particle dispersion and HYSPLIT backward-trajectory models. 2011. Journal of the Air & Waste Management Association, 61: 660-672.

Legg, B.J. and Raupach, M.R. 1982. Markov chain simulation of particle dispersion in inhomogenous flows: the mean drift velocity induced by a gradient in Eulerian velocity variance. Bound. Layer Meteorol., 24: 3-13.

Mellor, G.L. and Yamada, T. 1974. A hierarchy of turbulence closure models for planetary boundary layers. J. Atmos. Sci., 31: 1791-1806.

Nickling, W.G., Gillies, J.A., Berg, A. and Brown, L. 2010. A Feasibility Study for the Development of a RADARSAT-2 Dust Prediction System. Report Prepared for British Columbia Hydro, Richmond, BC, March 2010.

Nickling, W.G., Gillies, J., Brown, L.J. and Trant, J. 2011. A Feasibility Study for the Development of a RADARSAT-2 Dust Prediction System: 2010 Report.

Pielke, R.A. 1984. Mesoscale Meteorological Modeling. Academic: New York,.

Rodean, H. 1996. Stochastic Lagrangian models of turbulent diffusion. Meteorol. Mono., 26: 4740-4750.

Shao, Y. 2000. Physics and Modelling of Wind Erosion, 393 pp., Kluwer Academic Publishers, Dordrecht.

Shao, Y. 2004. Simplification of a dust emission scheme and comparison with data. Journal of Geophysical Research, 109 (D10202).

Sweeney, M. R. and A. Mason (2013). "Mechanisms of dust emission from Pleistocene loess deposits, Nebraska, USA." Journal of Geophysical Research-Earth Surface 118, 1-12,.

Sweeney, M., McDonald, E.V. and Etyemezian, V. 2011. Quantifying dust emissions from desert landforms. Geomorphology, 135; 21-34.

Sweeney, M., Etyemezian, V., Macpherson, T., Nickling, W.G., Gillies, J., Nikolich, G. and McDonald, E. 2008. Comparison of PI-SWERL with dust emission measurements from a straight-line field wind tunnel. Journal of Geophysical Research, Earth Surface, 113: F01012.

von Kármán, T. 1954. Aerodynamics. Cornell University Press, Ithaca. 203 pp.

Xiao, J., Shen, Y., Tateishi, R. and Bayaer, W. 2006. Development of a topsoil grain size index for monitoring desertification in arid land using remote sensing. International Journal of Remote Sensing, 27: 2411-2422.